Catena 217 (2022) 106434

Contents lists available at ScienceDirect

Catena

journal homepage: www.elsevier.com/locate/catena

Soil organic carbon stocks in the high mountain permafrost zone of the semi-arid Central Andes (Cordillera Frontal, Argentina)

Peter Kuhry [a,*], Eirini Makopoulou [a,1], Didac Pascual Descarrega [a,2], Ivanna Pecker Marcosig [b], Dario Trombotto Liaudat [b]

[a] Department of Physical Geography, Stockholm University, 106 91 Stockholm, Sweden
[b] Geocryology, Instituto Argentino de Nivología, Glaciología y Ciencias Ambientales, CONICET, Mendoza, Argentina

ARTICLE INFO

Keywords:
Soil organic carbon
Land cover
Landform
Mountain permafrost and periglacial zone
Andes
Global warming

ABSTRACT

This study presents the first detailed soil organic carbon (SOC) inventory for a high mountain permafrost zone in the semi-arid Central Andes of South America. We describe plant cover and soil profiles at 31 sites representing the main land cover and landform types in the Veguitas catchment (Cordillera Frontal, Argentina), which ranges in elevation from c. 3000 to 5500 m. The vegetated area with soil development is largely confined to altitudes of < 3650 m and represents only 8.2% of the total catchment area. Mean SOC 0–100 cm storage for the vegetated portion of the catchment is 3.62 kg C m^{-2}, which is reduced to 0.33 kg C m^{-2} if we consider negligible SOC stocks in the extensive bare ground and glaciated areas at higher elevations. Hotspots of SOC storage are wet meadow areas, with peat deposits up to 102 cm deep and a maximum observed total SOC storage of 53.07 kg C m^{-2}. These wet meadow areas, however, occupy only 0.11% of the total catchment area and their contribution to mean SOC storage is limited. Among soils at well-drained sites, highest mean SOC 0–100 cm storage is found on backslope positions of moraines that predate the Last Glacial Maximum (6.87 kg C m^{-2}). Only 2% of all SOC stocks in the catchment are found in permafrost terrain and none are located in the permafrost layer itself. The main ecoclimatic control on SOC storage is plant cover, with vegetation limits being sensitive to ambient temperature. Projected increases in temperatures will not remobilize any frozen SOC stocks but will likely result in an upward shift of the upper vegetation belt with soil development creating new areas of phytomass carbon and SOC storage. The area is expected to represent a net C sink and thus a negative feedback on future global warming.

1. Introduction

Gruber et al. (2004) identified permafrost as one of the vulnerable carbon (C) pools in the Earth System. Research in permafrost C was further stimulated by a new and very high estimate of soil organic carbon (SOC) storage in the northern circumpolar permafrost region (Tarnocai et al., 2009), which was updated in Hugelius et al. (2014). The latter assessment reports a SOC storage estimate of c. 1300 PgC for the c. 18 million km^2 of soil area in the northern permafrost region. Bockheim and Munroe (2014) reported c. 66 PgC in soils for the c. 3.6 million km^2 of global mountain permafrost area, about half of which is located outside the contiguous northern permafrost region.

The very large SOC stocks in permafrost regions have raised concerns regarding a positive permafrost C feedback on global warming. In recent years, comprehensive reviews have been published on the role of gradual permafrost thaw (active layer deepening) and abrupt permafrost degradation (e.g. thermokarst, thaw slumps) for C remobilization and release (Schuur et al., 2015; Turetsky et al., 2020). Much of these assessments have focused on lowlands in the northern permafrost region due to their large SOC stocks. In these areas, eventual gains in phytomass C due to an expansion of shrubs and trees into current arctic tundra are not expected to compensate for the large SOC losses following permafrost thaw (Abbott et al., 2016).

Hugelius et al. (2014) reported a paucity of data from mountain areas in the northern permafrost region. Bockheim and Munroe (2014) compiled published data on soil genesis and SOC storage in mountain

* Corresponding author.
E-mail address: peter.kuhry@natgeo.su.se (P. Kuhry).
[1] Present address: Geography Research Unit, P. O. Box 8000, FI-90014 University of Oulu, Finland.
[2] Present address: Department of Physical Geography and Ecosystem Science, Lund University, 223 62 Lund, Sweden.

https://doi.org/10.1016/j.catena.2022.106434
Received 13 July 2021; Received in revised form 16 May 2022; Accepted 4 June 2022

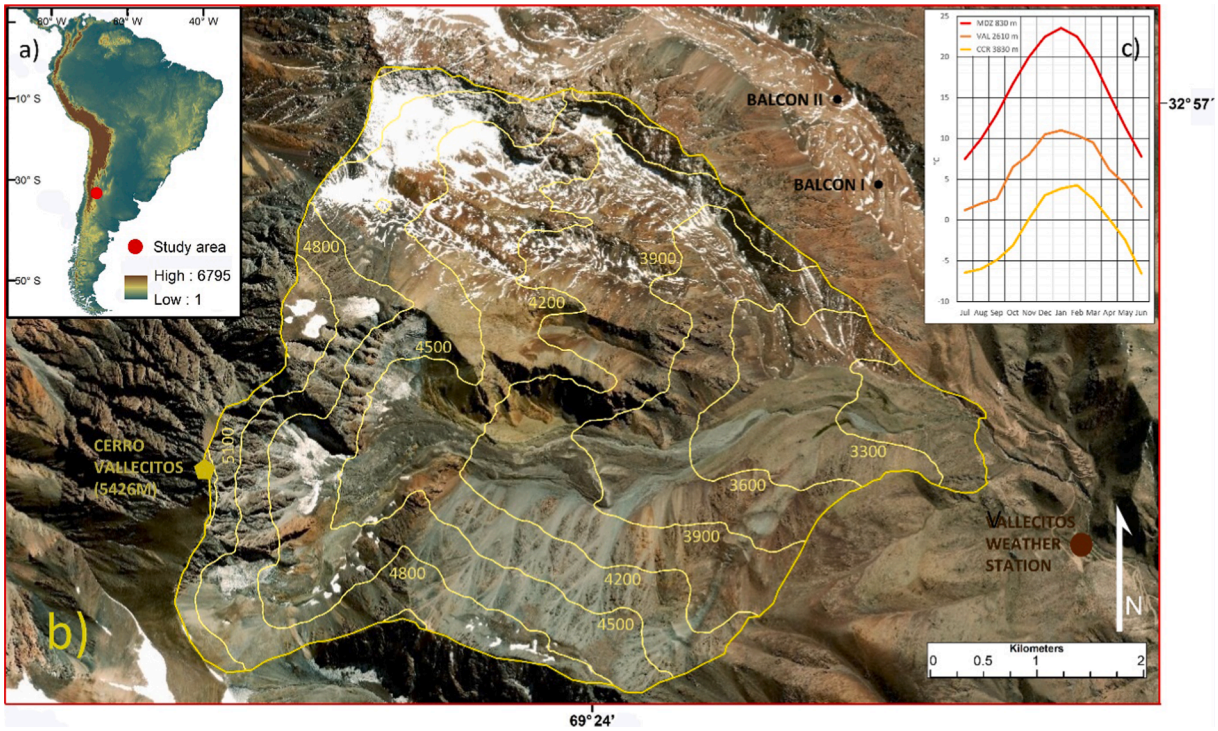

Fig. 1. a) Location of study area in S-America (red dot), map downloaded from https://earthexplorer.usgs.gov/; b) Google Earth view of the Veguitas catchment (delineated by yellow line) with 300 m contour lines, location of Vallecitos weather station down-valley and permafrost monitoring sites Balcon I and Balcon II in nearby Morenas Coloradas rock glacier, source background ESRI, DigitalGlobe, GeoEye, Earthstar Geographics, CNES/Airbus DS, USDA, USGS, AeroGrid, IGN, and the GIS user community; c) Mean monthly air temperatures at Cerro Cristo Redentor (CCR; 3830 m), Vallecitos (VAL; 2610 m) and Mendoza (MDZ; 830 m). (For interpretation of the references to color in this figure legend, the reader is referred to the web version of this article.)

permafrost regions from around the globe. Their review focused on vegetated areas with soil development but did not specifically address the extent or potential role of bare ground areas in high mountain permafrost settings. Mountain permafrost outside of the northern permafrost region represents an area of c. 1.5 million km^2. Much of this area corresponds to the Tibetan Plateau with c. 1.1 million km^2 (Zou et al., 2017), followed in extent by the Andes. According to Saito et al. (2015), the total area of Andean permafrost can be estimated at c. 136,000 km^2, which is both higher and lower than previous estimates (e.g., Gorbunov, 1978; Haeberli et al., 1993). The lower altitudinal limit of permafrost ranges from c. 4500 m in the arid Andes (15° S) to c. 1500 m in the humid Patagonian Andes (50° S). No previous SOC estimates are available for this large mountain permafrost area.

The key objectives of this study are to 1) obtain the mean and range of SOC storage in a mountain permafrost area of the semi-arid Central Andes, 2) describe physicochemical properties for a range of soil types, 3) assess topographic controls on SOC storage, 4) determine to what extent the upper vegetation belt with soil development overlaps with the mountain permafrost zone along an elevational gradient, and 5) evaluate the consequences of global warming and permafrost thawing on the future net C balance in this high mountain region.

2. Study area

The study area is located in the Parque Provincial Cordon del Plata, on the eastern flank of the Cordillera Frontal in the Central Andes near Mendoza, Argentina (Fig. 1a). The Veguitas catchment extends from c. 3000 to 5500 m elevation and drains an area of c. 28 km^2 (Fig. 1b). A portion of this area has been identified as the Infiernillo-Rincón Basin of the larger Vallecitos catchment in Sileo et al. (2020). Prominent landforms are the large, mostly debris-covered, Vallecitos glacier and the Infiernillo rock glacier in the central valley, and two other large rock glaciers (Franke and Stepanek) in adjacent valleys. Gelifluction lobes and patterned ground (stripes and sorted circles) were observed at c. 4150 m, with relict sorted circles at c. 3500 m.

Bedrock in the study area is composed of dark-colored metamorphic quartzites in the southern/central part of the study area, with reddish-brown volcanic rhyolites in the more northern sectors (Wayne and Corte, 1983). There is widespread evidence of multiple glacial advances in the Veguitas catchment during the Late Pleistocene and Holocene. An older glacier advance, which extended down-valley to c. 2600 m, predates the Last Glacial Maximum (pre-LGM). A conspicuous glacier advance to c. 3200 m is considered of LGM age (c. 19000 years ago). Multiple glacier advances are documented up-valley (>3500 m) for the Late Holocene Neoglacial period (<6000 years old). Rock glaciers at places overtop these Late Pleistocene and Neoglacial moraines and are considered of Holocene age (Wayne and Corte, 1983).

Climatically, the study area is located in the semi-arid Central Andes. There are few high-elevation weather stations in the region and their records are short and/or discontinuous. Fig. 1c presents mean monthly air temperatures for Cerro Cristo Redentor (32° 54′ S, 70° 12′ W; 3830 m), Vallecitos (32° 59′ S, 69° 21′W; 2610 m) and Mendoza (32° 54′ S, 68° 54′ W; 830 m), roughly representing the 2nd half of the 20th Century. Based on these observations we can infer a lapse rate in mean annual air temperatures of c. 0.6 °C / 100 m elevation. Mean annual air temperature in Mendoza has increased by c. 1.5 °C since the beginning of meteorological observations till present (1906–2018). Mendoza and Vallecitos receive c. 250 and 400 mm of annual precipitation, respectively, with most falling in the summer period from an Atlantic source, whereas Cerro Cristo Redentor has c. 270 mm of annual precipitation mostly falling in the winter season from a Pacific source. Snow cover has been monitored for 4 years (2018–2021) at the Balcon I permafrost monitoring site in nearby Morenas Coloradas rock glacier, located at 3560 m elevation (Fig. 1b). There is occasional snowfall (<1 cm) in January to May. The winter months are very dry and snow depth on average does not exceed 2 cm (observed max 4.2 cm) from June to

Fig. 2. Landscape images of the Veguitas catchment: a) Cerro Vallecitos (5426 m), with the debris-covered Vallecitos glacier in the forefront (c. 4300 m); b) Glacier cirques, steep bedrock and scree slopes in northwestern corner of the study area (photo site c. 4200 m); c) Campsite on high terrace of the Infiernillo glacio-fluvial floodplain, with LGM lateral moraine to the right (c. 3500 m); d) Lower reaches of the Stepanek rock glacier in the forefront (c. 3600 m), with LGM moraines in the Infiernillo valley and the Franke rock glacier on the opposite slope; e) Alpine meadows in the Veguitas area proper (c. 3250 m), with lateral and terminal moraines of LGM age; f) Tall shrubs on stony slopes with northeastern aspect in the lower reaches of the Veguitas catchment (c. 3100 m). (For interpretation of the references to color in this figure legend, the reader is referred to the web version of this article.)

December (D. Trombotto L. and I. Pecker M., personal communication, 2022). Meteorological data was obtained from KNMI Climate Explorer (http://climexp.knmi.nl), Mendez (2004), Mendez et al. (2006) and Trombotto and Borzotta (2009).

The zonal vegetation types in the Cordon del Plata, on the eastern flank of the Cordillera Frontal, are described by Mendez (2004). There is no mountain forest belt (and thus treeline) on the eastern slopes of Central Andes at these latitudes (between c. 29-38° S), as is the case in many arid mountain regions of the world (Hoffmann, 1982). In the upper Andean belt, zonal vegetation is characterized by shrubs of *Adesmia horrida* with an understory of grasses up to c. 3200 m, by dwarf shrubs of *Adesmia hemisphaerica* and/or woody cushion plants of *Adesmia subterranea* and *Azorella monantha* with grasses up to c. 3700 m, and very sparse vegetation with forbs up to c. 4200 m. In our study area, we observed tall *Adesmia* shrub communities (canopy height $\leq$ 100 cm) on steep, stony slopes with a northern aspect up to c. 3250 m, dwarf shrub-grass-cushion plant communities on stable moraine and rock glacier slopes up to elevations of c. 3650 m, with single individuals of vascular plants in protected rock crevasses up to c. 3900 m, and epilithic lichen up to c. 4150 m. Mendez et al. (2007) describe azonal meadows (local names: mallines, vegas, diminutive: veguitas, or bofedales) in the study area up to c. 3300 m. They are found on glacio-fluvial floodplains along streams supplied by water discharge from glaciers and rock glaciers. Similar meadows are described from the nearby Aconcagua

Provincial Park up to elevations of c. 3800 m (Barros et al., 2014). They are characterized by a dense cover of grasses, sedges and/or rushes (e.g. *Deyeuxia vellutina, Carex Gayana, Patosia clandestina*). There is very limited data on above-ground phytomass in these plant communities. Using allometric equations based on shrub height and diameter of *Adesmia volckmannii* shrubs in dry Patagonian steppe (Oñatibia et al., 2010), we can estimate an above-ground biomass of c. 0.5–2 kg C m^{-2} in the shrub and dwarf shrub-grass-cushion plant communities of our study area. Barros et al. (2014) give a range of 0.8–1.0 kg C m^{-2} for grazed meadows in Aconcagua Provincial Park. The plant communities in the Veguitas study area are grazed by wild Guanaco (*Lama guanicoe*), and a few cows and horses.

The lower limit of permafrost in the study area was observed in the terminus of the Stepanek rock glacier at c. 3350 m. The Franke and Infiernillo rock glaciers extend down to c. 3450 and 3600 m, respectively. Two small rock glaciers terminate at c. 3650 m. The upper layer of debris on these rock glaciers provides insulation for the underlying (creeping) permafrost body. More extensive mountain permafrost (continuous, *in situ* aggraded) is probable above an elevation of c. 3800–3900 m, which corresponds to the current location of the zero annual isotherm (Trombotto et al., 2020). Permafrost monitoring is ongoing in the nearby Morenas Coloradas rock glacier (see Fig. 1b). Trombotto and Borzotta (2009) report deepening active layers at the Balcon I (3560 m) and Balcon II (3770 m) sites, which they relate to ongoing climate warming.

The predominant soils in the study area have poorly developed soil genetic horizons, high stone content and shallow regolith, typical of this type of high mountain environment. Evidence for permafrost in the form of ground ice was not encountered in any of the collected soil profiles, even in the inactive part of a rock glacier where the permafrost layer is most likely located at depths > 2 m (Trombotto and Borzotta, 2009). These soils can be classified as Leptosols and Regosols (IUSS Working Group WRB, 2006). In glacio-fluvial floodplain deposits, soils are classified as Fluvisols. The soils in wet meadows are organic-rich, with often buried peaty layers. Some of the soils can be classified as Histosols because peat depth exceeds 40 cm. In other cases, the soils can be considered Histic Gleysols. Soils at higher elevations, affected by gelifluction and cryoturbation, have likely permafrost in the upper 2 m of the profile and can be classified as Turbic Cryosols. However, there is very limited plant cover and soil development in the study area above c. 3650 m of elevation. Wayne and Corte (1983) used soil characteristics and weathering degree for relative dating of the moraine complexes in the study area. Soils were classified as Mollisols (pre-LGM and LGM moraines) and Inceptisols or Entisols (Holocene moraines), using USDA soil taxonomy (Soil Survey Staff, 2014).

Fig. 2 presents an overview of the overall setting of the Veguitas catchment study area, from highest peak (5426 m) to the lower limit (c. 3000 m) at the confluence with the main Vallecitos valley.

3. Methods

3.1. The field campaign

Following an initial field reconnaissance, three transects between 0.4 and 1.1 km length were set out that crossed all major land cover and landform types in the lower part of the Veguitas catchment (November-December 2017). In total, 31 soil profiles were described (29 sampled) between 3000 and 3700 m corresponding to the elevational range of the upper vegetated belts with soil development in the study area. Along transects, soil profiles were collected at strictly pre-defined, equidistant intervals (50 or 100 m) as determined by a handheld GPS. This semi-random sampling scheme ensures that all major landscape elements of interest are sampled but avoids any bias in exact profile site location. At each site, we described plant cover, fractions of large stones and of fine-grained mineral bare ground at the surface, landform and topography (elevation, slope and aspect). Plant cover was described by estimating cover of various plant functional types in different vegetation strata (tall shrub ≥ 25 cm, dwarf shrub < 25 cm, graminoids and forbs, cushion plants, mosses and lichen, etc). Because of overlapping strata, total coverage can exceed 100%. Higher elevation areas were photographed during hikes (up to 4500 m) to properly document bare areas without soil development in high mountain terrain. Raw field data from profile sites along the three transects is summarized in Table A1 of the Appendix.

Sampling at each site was carried out (nearly) continuously along the excavated soil pit, by cutting out and measuring the dimensions of blocks from the topsoil organic layer (if present), and by using a fixed volume cylinder or by coring with a fixed diameter steel pipe in deeper soil layers. Volume estimates of large stones (≥4 cm in diameter) were made for the surface (radius of 5 m around the profile site) and for each sampled depth interval (CF_{large}, volume %). At those sites where a topsoil organic horizon was present, three randomly selected replicates were collected to acquire a more representative sample. A 100 cm^3 cylinder was used to collect samples below the top organic layer in shallow and stony soils to as deep as bedrock or stony regolith allowed. In deep and fine-grained profiles, deeper samples were retrieved every c. 10 cm by incrementally hammering a steel pipe into the ground until bedrock/large stones were hit. For every sample, additional metadata was collected including exact depth interval, soil texture and color, occurrence of roots, and presence of small stones (<4 cm). Collected soil profiles were generally shallow and the standard soil reference depth of 100 cm was only reached at two locations. Evidence for permafrost was not encountered in any profile.

In total, 156 soil samples were collected. Another six samples of large stones were taken to estimate the mean dry bulk density of the coarse fraction. This allowed to recalculate weight fraction of small stones in soil samples into volume estimates. Five woody root samples were collected to estimate their bulk density and carbon content. This permitted to calculate the contribution of large woody roots recorded in two soil profiles (four depth intervals) to total C stock in the samples. In one of these profiles, the roots were described as large 'living' roots. Additional observations on root penetration into glacio-fluvial materials underlying a soil profile were made at a natural exposure in the study area. Ten samples were used for radiocarbon dating. Six of these samples correspond to peat(y) layers in wet meadow profiles and another three to root samples in soil profiles at well-drained sites. One soil sample of a B-horizon has also been used for dating purposes. The dates on peat(y) samples were used to establish the age of buried layers and calculate peat accumulation rates. The dates on deep (dead, decomposing) roots and organic matter in a B-horizon were submitted to obtain a rough indication of the age of some of the oldest organic C preserved in the mineral upland soils.

3.2. Laboratory analyses

Soil samples (n = 156) were weighed in the laboratory before and after oven drying at 65 °C for 4 days to calculate their gravimetric water content (% weight) and dry bulk density (DBD, g cm^{-3}). Subsequently, all samples with a coarse fraction were sieved through a 2 mm mesh in order to measure the small stone fraction in the sample (CF_{small}, % weight). Loss on ignition at 550 °C for 5 h (LOI550, % weight) was used to estimate the soil organic matter (SOM) content in each of the samples (Heiri et al., 2001). For those few depth increments from which no samples were taken, soil properties were interpolated from adjacent samples, considering any relevant field observations such as soil texture, percentage of stones, root occurrence, etc.

A total of 68 samples from seven profiles, selected to represent the different land cover classes in the study area, were also burnt at 950 °C for 2 h (LOI950, % weight) to estimate inorganic carbon content (Heiri et al., 2001). Every other sample from the same profiles (n = 35) were processed in a Carlo Erba Elemental Analyzer NC2500 attached to a Finnigan MAT Delta Plus mass spectrometer to determine their total C

and N contents, and $\delta^{13}C$ and $\delta^{15}N$ isotopic signals. A further subset of 13 samples from two of these profiles were re-sampled, acid-treated with HCl, and re-analyzed to assess whether any inorganic carbon might be present in these soil profiles. Neither the LOI at 950 °C nor the %C or $\delta^{13}C$ signatures in acid-treated samples provided any indication for inorganic carbon in samples, which is considered negligible in our subsequent estimates of SOC stocks in soil profiles. Equation (1) ($n = 32$, $R^2 = 0.97$, $p < 0.05$) shows the 3rd order polynomial regression model, based on individual samples for which both %C and LOI at 550 °C values were available, used to calculate the %C for the depth increments where only LOI at 550 °C data was available. A polynomial fit is necessary in order to properly represent (and not overestimate) %C in mineral subsoil samples with low LOI550 values (Fig. A1 in the Appendix).

$$\%C = 0.000081*LOI550^{(3)} - 0.006667*LOI550^{(3)} + 0.537323*LOI550 - 1.130646 \quad (1)$$

Ten samples were submitted for AMS ^{14}C dating to the Radiocarbon Laboratory in Poznan, Poland. The resulting ages in ^{14}C yr BP, were calibrated to calendar years, cal yr BP (1950), using OxCal 4.4 (Bronk Ramsey, 2009) and the Southern Hemisphere SHCal20 calibration curve (Hogg et al., 2020) or, in the case of 'modern' ages, to AD years using the Southern Hemisphere Bomb13SH12 calibration curve (Hua et al., 2013).

3.3. SOC storage calculations

The SOC content (kg C m^{-2}) for each sample was calculated using Equation (2), where CF_{large} is the volume fraction of large stones (>4 cm) described from the soil pits, *DBD* (g cm^{-3}) is the dry bulk density of the sample, *%C* is the weight fraction of carbon in the sample, CF_{small} is the weight fraction of the small stones (>2 mm) in the sample, *D* is the depth interval of the sample (cm), and *10* is for unit conversion:

$$SOC_{sample} = (1 - CF_{large})*DBD*\%C*(1 - CF_{small})*D*10 \quad (2)$$

For profiles with topsoil organics, SOC stocks in this layer are calculated as the mean of the three collected replicates. SOC storage in soil profiles was calculated for the standard intervals of 0–30 cm and 0–100 cm, by adding up SOC stocks of each sample down to these depths. In all but two soil profiles the depth of 100 cm was not reached due to the presence of large stones or bedrock. The interval between the depth at which sampling was stopped due to stones and 30 cm or 100 cm was assumed to contain negligible SOC. SOC calculations were performed for the entire study area and its vegetated fraction, since SOC storage is largely expected under vegetated areas only. Especially in high mountain terrain, but also at lower elevation on steep slopes, active rock glaciers and active floodplains, soil development was negligible.

3.4. Digital elevation model and land cover classification

Elevational gradient analyses for the study area are based on a digital elevation model (DEM) using ALOS PALSAR data from 2011 (12.5 m resolution). The DEM is used to assess the altitudinal distribution range of different land cover classes in the Veguitas catchment and to generate contour lines for mapping and analysis purposes.

A land cover classification (LCC) for the 28 km^2 study area was derived from a WorldView2 satellite image acquired the 18th of March 2017 (0.5 m resolution). A maximum likelihood supervised classification (Campbell and Wynne, 2011) was applied using the spectral bands 2–6, the NDVI index and the true color WorldView2 image. We distinguish five different land cover classes, i.e. snow-ice-water, bare, sparse, shrub and meadow. The NDVI values for each class are as follows: water < 0, snow/bare 0–0.1, sparse 0.15–0.3, shrub 0.4–0.5 and meadow 0.6–0.8 (Jones and Vaughan, 2010).

The training set for the different land cover classes consisted of 31 vegetation descriptions at our soil profile sites, and an additional 46 sites picked from the study area and the larger region covered by the WorldView2 image that unambiguously correspond to one of these land cover classes. Of these, 21 georeferenced points are based on photographic evidence collected during hikes in the study area. This resulted in a total of total 77 ground truth points, with a minimum of 10 points per class. A Kappa index of agreement and Overall accuracy were calculated from a confusion matrix.

3.5. LCC-based upscaling and topographic controls of SOC stocks

The SOC storage 0–30 cm and 0–100 cm in all soil profiles belonging to the same land cover class were averaged to obtain mean SOC kg C m^{-2} storages (and their standard deviation) per land cover class. These values were then weighed by the proportion of area covered by each land cover class to estimate mean SOC 0–30 cm and 0–100 cm storages in the Veguitas catchment and its vegetated fraction only. The land cover classes ice-snow-water and bare > 3900 m were assumed to contain negligible SOC.

SOC storage in soil profiles were also assessed as a function of elevation, slope and aspect both for the full data set ($n = 31$) as well as for well-drained sites only ($n = 21$). In the latter case, soil profiles in active floodplain ($n = 4$) and wet meadow ($n = 6$) areas were excluded. These are generally confined to a narrow elevation range (mostly 3200–3300 m) and relatively flat areas (mostly 0-3°) and have negligible to very high SOC storage that would obscure topographic controls on SOC storage for the remaining well-drained sites. In the case of aspect, we define the slope orientation of a site as degrees deviation from North (South is 180°, West and East are both 90°, etc.). We also calculated mean SOC storage for each 100 m elevation interval focusing on the lower portion of the Veguitas catchment (3000–4200 m), by multiplying mean storage of each land cover class by their proportional representation in each elevation interval. For moraine sites ($n = 11$), we conducted an additional analysis of SOC storage as a function of catenary position.

3.6. Statistical analyses

To obtain error estimates for SOC storage in the study area as a whole and its vegetated fraction, 95% confidence interval (CI) ranges were calculated using Equation (3), where: *t* is the upper α/2 of a normal distribution ($t = 1.96$), *ai* is the total areal extent (%) of the upscaling unit i, *SDi* is the standard deviation of the upscaling unit i, and *ni* is the number of replicates in class i (Thompson, 1992). CI ranges presented here are only an indicator of uncertainties caused by proportion of area, variability in SOC stocks and/or low number of replicates in each class, but do not account for errors in the upscaling products (Hugelius, 2012).

$$CI = t^*\sqrt{\sum\left(\frac{(ai^2*SDi^2)}{ni}\right)} \quad (3)$$

Relationships between SOC storage, plant cover, soil depth and topography are analysed using 2nd and 3rd order polynomial regressions in the Microsoft Excel 2010 and Past3 (Hammer et al., 2001) software packages. Regressions are considered significant if $p < 0.05$.

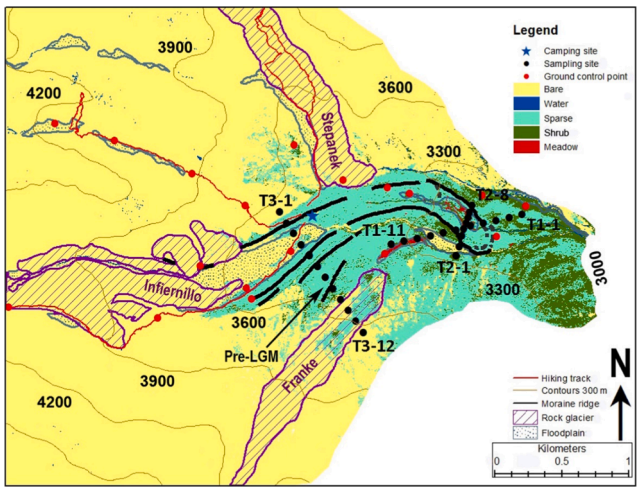

Fig. 3. Land cover map of the lower section of the Veguitas catchment, with location of transects and soil profile sites and hiking trails into high mountain terrain (with additional ground truth points). Hiking trails and transect 3 were reached from the camping site, whereas transects 1 and 2 were accessed daily from the nearby Refugio San Bernardo (c. 2800 m). Large landforms such as prominent rock glaciers, active floodplains, and moraine ridges are given for reference, highlighting the location of the pre-LGM moraine described in Wayne and Corte (1983). (For interpretation of the references to color in this figure legend, the reader is referred to the web version of this article.)

4. Results

4.1. Land cover classification

The supervised land cover classification scheme has a very high Overall Accuracy (0.94) and Kappa index of agreement (0.92). The underlying reason is that we only distinguish five land cover classes, of which the classes snow-ice-water, meadow and bare have very distinct spectral properties and are correctly identified in 100% of ground truth cases. There is some misclassification between the shrub and sparse classes (15% of cases), which show overlap in land cover characteristics.

The upper reaches of the Veguitas catchment are characterized by bedrock, bare ground, glacier ice and perennial snow patches, without any plant cover and soil development. The distribution of land cover classes in the lower portion of the Veguitas catchment is depicted in Fig. 3. At these lower elevations, the class snow-ice-water is represented by open water in streams. The vegetated classes meadow and shrub are largely restricted to elevations of < 3400 m, whereas sparse is common up to c. 3650 m. The classes meadow and bare, with 98 ± 5 and 4 ± 6% plant cover (mean and standard deviation), respectively, form very distinct groups. Meadows are restricted to areas with gentle slopes (≤8°), but bare areas occur on flat, active floodplains, on active rock glaciers and on steep slopes below the vegetation limit (as well as higher elevations). The difference in plant cover between the classes shrub and sparse (59 ± 6 and 58 ± 17%, respectively) is minimal. The shrub class is based on signatures from tall shrub stands at lower elevations (<3300 m), which were all correctly identified in the classification scheme. However, some areas at higher elevation (but below the vegetation limit of c. 3650 m) were also assigned to the same class. Overall, the two classes differ in the cover of (dwarf-) shrubs (15 ± 11 and 5 ± 6%, respectively) as well as exposed fine-grained mineral ground (9 ± 6 and 29 ± 16%, respectively), which might be the reason they could be separated in the remote sensing analysis. While the cover of grasses in the shrub and sparse classes is similar (19 ± 3 and 16 ± 5%, respectively), the cover of cushion plants is greater in the sparse class (14 ± 13 and 24 ± 18%, respectively). Large stones at the surface are much more common in the shrub than sparse class (35 ± 15 vs 18 ± 7%). The shrub class is restricted to steep slopes (23 ± 3°) with a N to NE aspect, whereas the sparse class occurs along a range of slopes (9 ± 10°) and aspects (N to S). Examples of land cover classes are shown in Fig. 4.

4.2. Soil profiles

Stable ground surfaces were observed above the vegetation limit, e.g. on lateral moraines of Holocene (Neoglacial) age (Fig. 4a) and on inactive outwash plains with patterned ground such as sorted circles (Fig. 4b). This type of sites currently do no hold any SOC stocks but are potentially suitable for vegetation establishment and soil development under a future warmer climate.

Soil profile sampling focused on areas below the current vegetation limit at c. 3650 m. Fig. 5 presents key physicochemical variables for selected soil profiles representing the three vegetated land cover classes sparse, shrub and meadow. Table 1 shows the results of radiocarbon dating of selected soil profiles and samples. Soil development in the sparse and shrub classes was largely restricted to the upper 40 cm of the profiles, whereas meadow profiles were between 40 to > 100 cm deep. The meadow profiles, located in relatively flat areas with poor water drainage, were generally less stony and much wetter, with lower dry bulk density, and higher %C and C/N ratio, than the sparse and shrub class profiles, located in well-drained sites. Steep (talus) slopes (Fig. 4c), active floodplains and the surface of active rock glaciers (Fig. 4d), even when located below the vegetation limit, were largely bare and had no soil development.

Soil profiles T3-10 and T3-11 were located on the lower reaches of the Franke rock glacier, the first on the steep slope of the rock glacier terminus, the second on a stable surface of the inactive part of the rock glacier. The sites must be underlain by permafrost but the perennially frozen layer was not reached in either profile. Site T3-10 had very limited plant cover and a negligible SOC storage of 0.02 kg C m^{-2} (not shown), whereas site T3-11 had a sparse vegetation cover of dwarf shrubs, grasses and cushion plants (Fig. 4f) and a SOC storage of 3.56 kg C m^{-2} (Fig. 5).

The soil with the highest SOC storage in a well-drained setting is T3-7 (7.09 kg C m^{-2}), located on the backslope of a pre-LGM moraine. Vegetation at the profile site was classified as sparse and was dominated by cushion plants, with dwarf shrubs and grasses. The soil profile was relatively deep (46 cm), with few large but many small stones, and slightly elevated %C and C/N values compared to most other soil profiles in well-drained settings (Fig. 5). Soil organic matter in the B-horizon of this profile (excluding living roots) at 13–16 cm depth was dated to 501 cal yr BP. A dead, decomposing, woody root fragment at c. 35 cm was 'modern' in age (Table 1). Soil profile T3-8, on the same pre-LGM moraine, also adheres to these characteristics. Although relatively shallow (25 cm), it also has relatively high %C in mineral soil horizons resulting in a SOC storage of 6.65 kg C m^{-2} (not shown).

Soil profiles at other well-drained sites, like LGM moraines (T3-2, T3-6) and stable mountain slopes (T1-2, T1-3) were generally shallower with lower SOC contents. They are classified both as shrub and sparse in the land cover classification (Fig. 4h-j). Sites included in Fig. 5 have a SOC storage range of 1.82–4.44 kg C m^{-2}, the full range in the Veguitas dataset is 0.62–5.73 kg C m^{-2} (excluding the pre-LGM moraine sites described above).

A deep profile could be described from site T3-3 and the nearby margin of the glacio-fluvial high terrace. Patterned ground had developed in the terrace surface, with a sparse plant cover of cushion plants and some grasses currently covering the center of relict sorted circles (Fig. 4g). Soil development was mostly restricted to the upper 13 cm of the profile consisting of finer-grained material. Some root material was also observed in finer-grained sediment at 43–63 cm depth of the exposure. Total SOC storage is 3.42 kg C m^{-2} (Fig. 5). This soil likely postdates the development of the sorted circles. Radiocarbon dates on root material at 10–20 and 43–63 cm depths yielded 'modern' ages (Table 1).

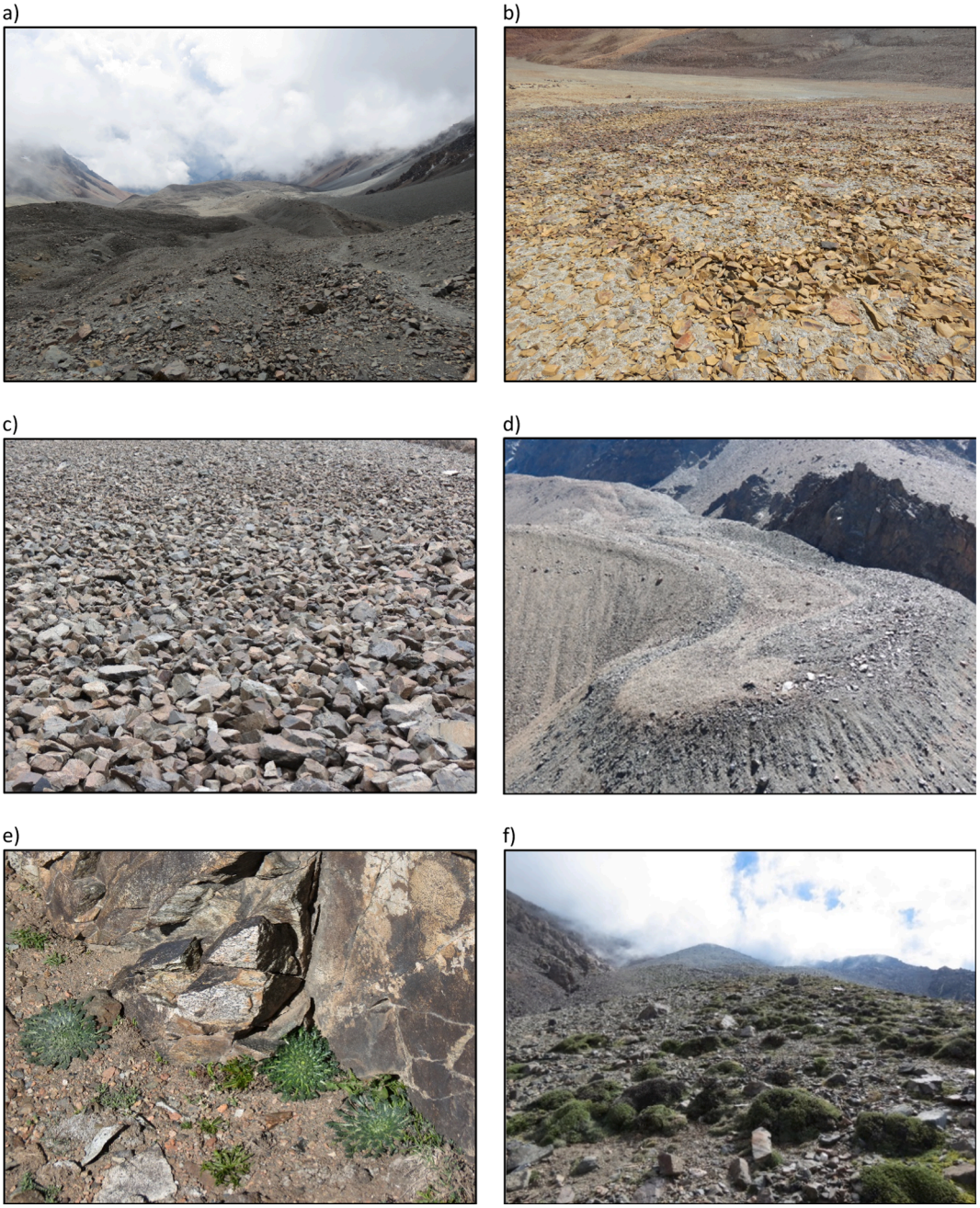

Fig. 4. Main land cover classes (and some landform types) in the Veguitas catchment: a) bare ground on Holocene moraine (right) and rock glacier (left) between c. 4000–4200 m; b) bare, patterned ground (sorted circles) on outwash plain at c. 4150 m; c) bare ground on active talus slope at c. 3600 m; (d) bare ground on active part of Stepanek rock glacier at c. 3400 m; e) patch with some vascular plants in-between block field at c. 3650 m; (f) sparse vegetation on inactive part of Franke rock glacier at c. 3550–3600 m. (g) sparse cushion plant vegetation on relict patterned ground (sorted circles) on high terrace of floodplain at c. 3465 m; h) sparse dwarf shrub vegetation on LGM moraine at c. 3400 m; (i) shrub vegetation on slope at c. 3200 m; j) sparse cushion plant vegetation on LGM moraine at c. 3200 m; k) meadow vegetation with water supply from Franke rock glacier at c. 3250–3300 m; (l) meadow vegetation in Veguitas area proper with water supply from upstream glaciers and rock glaciers at c. 3250 m. (For interpretation of the references to color in this figure legend, the reader is referred to the web version of this article.)

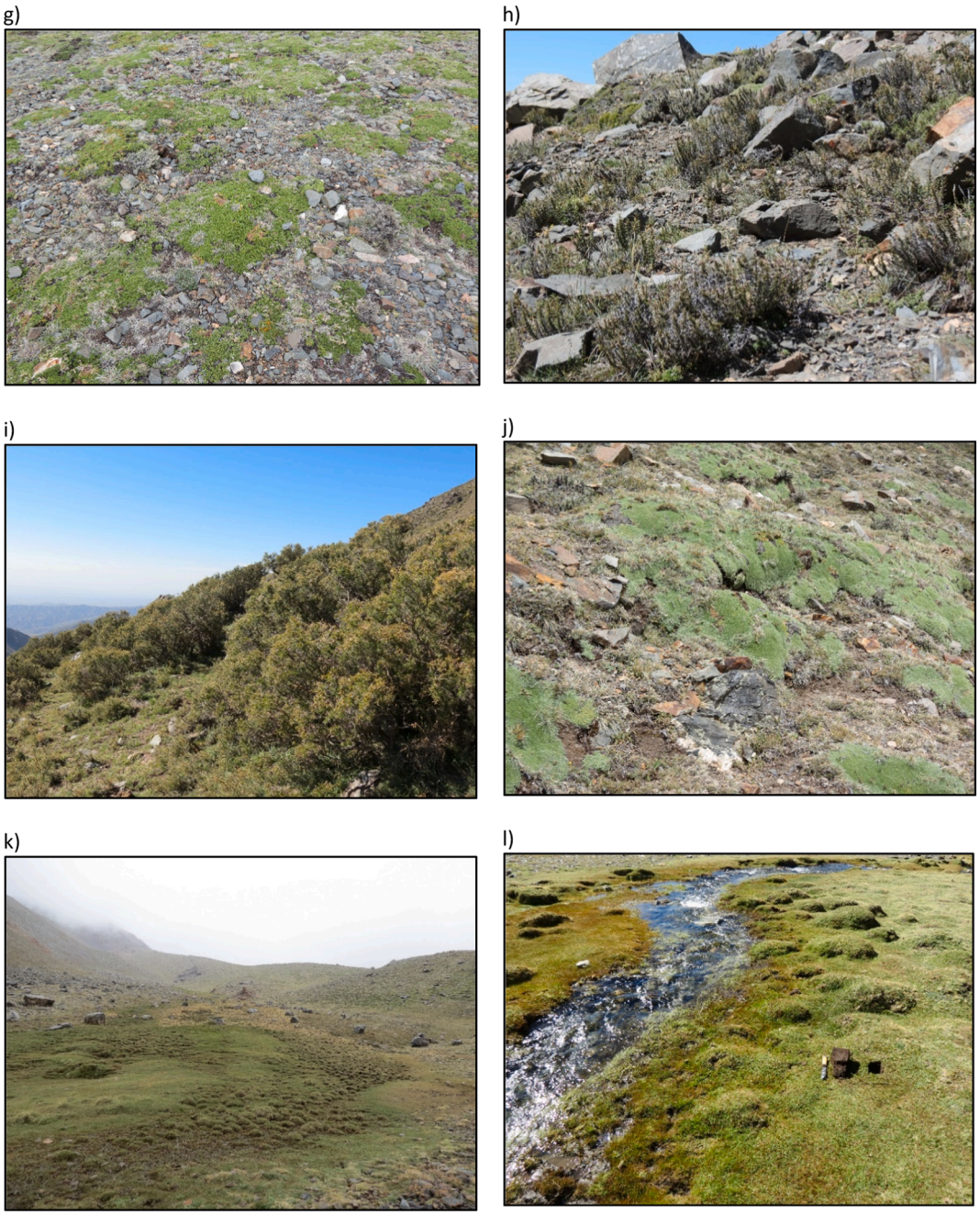

Fig. 4. (*continued*).

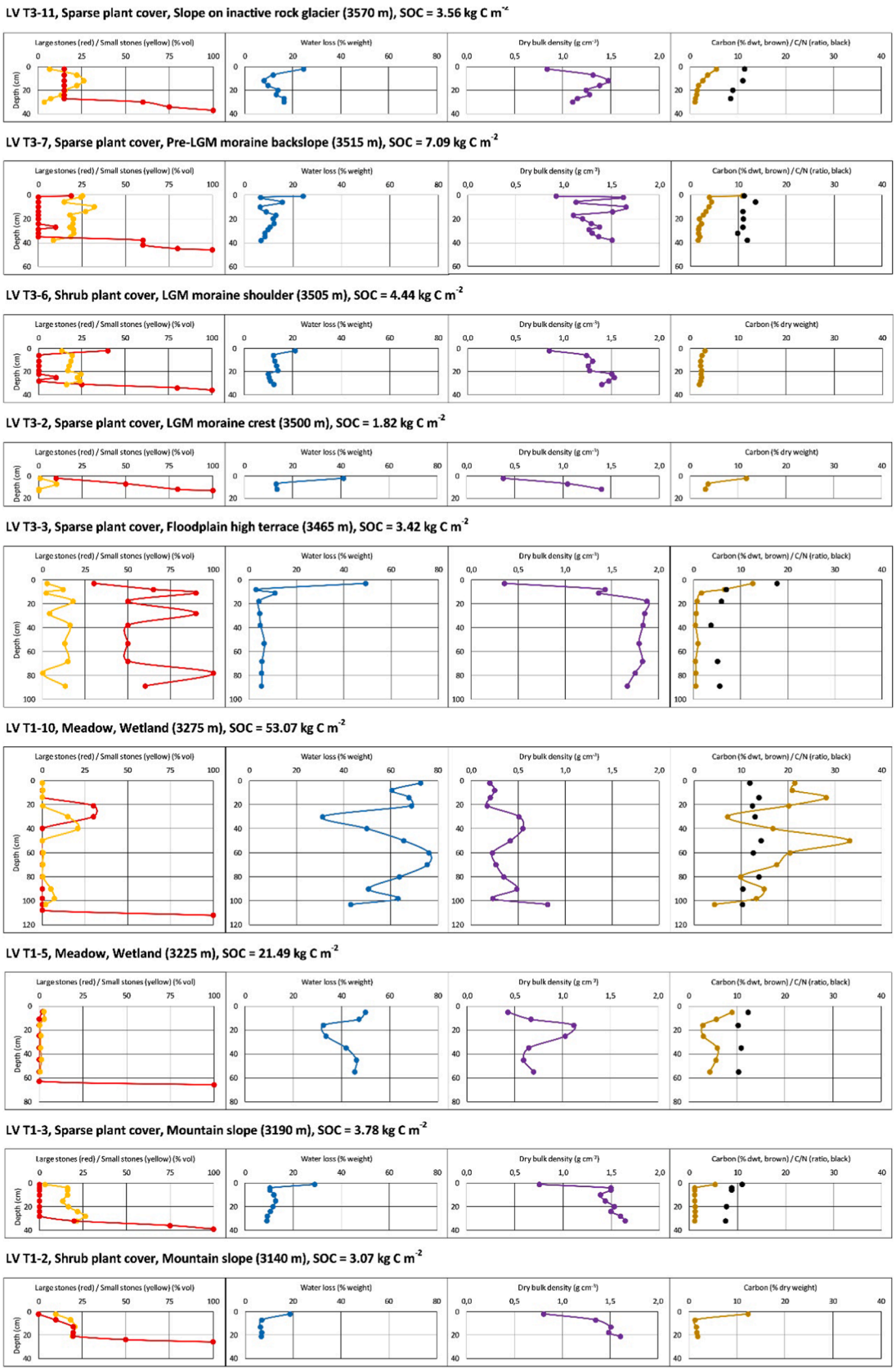

Fig. 5. Physicochemical properties of selected soil profiles, with land cover class, landform, elevation and total SOC storage. (For interpretation of the references to color in this figure legend, the reader is referred to the web version of this article.)

Table 1
Radiocarbon dates of selected soil samples reported as ^{14}C ages and calibrated ages.

Poznan Lab Number	Land cover	Profile	Depth (cm)	Horizon	Material	Age ^{14}C yr BP	Age cal yr BP * Modern AD
Poz-104124	Meadow	LV T1-5	12–13	Basal top organics	Plant remains	102.3 ± 0.38 pMC	1956AD
Poz-104125	Meadow	LV T1-5	51–52	Buried organic-rich	Bulk	1210 ± 30	**1072**, 1004, 1169, 1147
Poz-104126	Meadow	LV T1-10	20–22	Upper peat	Bulk	110 ± 30	**47**, 126, 90, 235
Poz-104127	Meadow	LV T1-10	49–51	Middle peat	Bulk	160 ± 30	**88**, 242, modern, 138
Poz-104128	Meadow	LV T1-10	101–102	Basal peat	Bulk	335 ± 30	**420**, 318, 381
Poz-104129	Meadow	LV T2-7D	23–24	Basal top organics	Bulk	60 ± 30	**43**, 125
Poz-132801	Sparse	LV T3-3B	10–20	Mineral subsoil	Woody root	128.45 ± 0.43 pMC	1979-1980AD
Poz-132881	Sparse	LV T3-3B	43–63	Mineral subsoil	Roots	103.79 ± 0.31 pMC	1956AD
Poz-132882	Sparse	LV T3-7	13–16	Mineral subsoil	B-horizon	470 ± 30	**501**
Poz-103152	Sparse	LV T3-7	35	Mineral subsoil	Woody root	110.39 ± 0.36 pMC	1998-2000AD

* Mean of 68.3% age ranges in decreasing order of probability (highest probability mean age in bold).

Table 2
Site properties and SOC storage (kg C m^{-2}) for the 0–30 cm and 0–100 cm depth intervals for each land cover class (mean and standard deviation), and weighed by proportional representation of land cover classes for total study area and vegetated area only (mean and confidence interval).

Land cover	Area (km^2)	% of total catchment	% of area vegetated	Sites (n)	Plant cover (%)	Soil depth (cm)	SOC 0–30 cm (kg C m^{-2})	SOC 0–100 cm (kg C m^{-2})
Meadow	0.03	0.11	1.36	6	98 ± 5	63 ± 28	11.3 ± 0.9	23.1 ± 13.4
Shrub	0.55	1.99	24.3	4	59 ± 6	27 ± 7	4.0 ± 2.0	4.1 ± 2.0
Sparse *	1.69	6.11	74.4	14	58 ± 17	23 ± 11	2.9 ± 1.6	3.1 ± 1.7
Bare < 3900	4.21	15.2	–	7	3.6 ± 5.8	1.6 ± 4.2	0.1 ± 0.1	0.2 ± 0.3
Bare > 3900	19.5	70.3	–	0	0	0	0	0
Snow-ice-water	1.72	6.23	–	0	0	0	0	0
Total study area	27.7	100	–	31	4.9	2.3	0.28 ± 0.07	0.33 ± 0.08
Total vegetated	2.27	8.22	100	24	59	25	3.28 ± 0.78	3.62 ± 0.83

* the sparse class includes one soil profile (T1-4) with 3% large living root volume described for the depth interval 5–13 cm, which accounts for c. 10% of its total SOC stock (0.40 kg C m^{-2} from a total of 3.91 kg C m^{-2}). Subtracting this root component from the SOC stock at this site reduces the mean SOC stock for the class by c. 1%, with negligible effects on total study area and total vegetated area SOC stocks.

Meadow profiles are characterized by C-rich materials at the surface and buried at greater depths. There are two main areas, one below the terminus of the Franke rock glacier (Fig. 4k) and the other one in the Veguitas area proper (Fig. 4l). These are wetland areas fed by water discharge that persists over the warm season from up-valley rock glaciers and glaciers. Plant cover is characterized by low, dense mats of graminoids of intense yellow or green colors that make them easily distinguishable both in the field and on remote sensing images. Their total SOC storage ranges between 11.63 and 53.07 kg C m^{-2}.

In the Franke rock glacier area, soils at two described meadow sites (T1-9 and T1-10) have thick sequences (75 and 112 cm deep, respectively) with > 40 cm peat, and can be considered Histosols. Stone- and/or finer-grained mineral-rich layers were observed intercalated in the peat layers at 34–40 cm (T1-9), at 24–35 cm in a nearby, small exposure (T1-9B), and at 26–35 and 75–85 cm (T1-10). In the Veguitas area proper, the four described meadow profiles (T1-5, T2-5, T2-6 and T2-7) were between 40 and 66 cm deep with thin topsoil organic-rich layers that in some cases adhere to the definition of histic horizon. Mineral subsoil at some meadow sites (T1-9B, T1-10 and T2-6) was described as clayey and/or displayed gleyic features in the form of iron mottling. Site T2-6 can, therefore, be classified as a Histic Gleysol. The %C values in the 66 cm deep T1-5 site do not exceed 9% (topsoil layer), but particularly low C content is found in the 13–30 cm depth interval (Fig. 5).

A total of six radiocarbon dates are available from three meadow profiles (Table 1). It should be acknowledged that many of these young ^{14}C dates provide multiple options for calibrated ages, which create large uncertainties in C accumulation rates depending on which calibrated age is used. Here, we base our calculations on the mean age of the highest 68.3% probability interval in the radiocarbon calibration. The oldest age is found for the C-enriched basal deposit at site T1-5 but is still young with a calibrated age of 1072 cal yr BP. The basal layer for the much deeper peat deposit at T1-10 is dated to only 420 cal yr BP. Using C stocks and basal dates (adding 67 years for the period 1950–2017) we obtain net C accumulation rates of 16.1 gC m^{-2} yr^{-1} for profile T1-5 and 101.5 gC m^{-2} yr^{-1} for profile T1-10. Recent accumulation rates can be derived from dates of the top peat(y) layer in the three meadow profiles. The 'modern' date of sample T1-5 12–13 cm can be assigned a likely age of 1956AD. Using again highest probability ages, we obtain recent C accumulation rates of 71.3 gC m^{-2} yr^{-1} for the top 12.5 cm of T1-5, 81.7 gC m^{-2} yr^{-1} for the top 21 cm of T1-10, and 37.3 gC m^{-2} yr^{-1} for the top 24 cm of T2-7D, corresponding to the last 60–115 years of meadow development.

Soil depth at individual profile sites is positively correlated with plant cover in the full Veguitas dataset ($R^2 = 0.69$, $p < 0.05$). Soil depth is a good predictor of total SOC storage ($R^2 = 0.94$, $p < 0.05$). Plant cover is positively correlated with SOC 0–30 cm ($R^2 = 0.86$, $p < 0.05$) and SOC 0–100 cm ($R^2 = 0.60$, $p < 0.05$). Correlations between soil depth and plant cover with SOC storage remain significant when removing the deep and SOC-rich meadow site T1-10 from the analyses ($R^2 = 0.84$–0.85, $p < 0.05$). Regressions are shown in Fig. A2 of the Appendix.

4.3. SOC upscaling

Table 2 shows the different land cover classes and their area, plant cover and soil attributes in the Veguitas catchment. The vegetated area

Table 3
Site properties and mean and standard deviation of total SOC storage (kg C m^{-2}) for the full depth of soil profiles for different landform types below the vegetation limit (<3650 m). Bare ground is mineral surface with grain size < 4 cm and large stones have grain size ≥ 4 cm.

Landform classes	Number of sites	Slope (degrees)	Bare ground cover (%)	Large stone cover (%)	Soil depth (cm)	Total SOC (kg C m^{-2})
Active slope	4	31 ± 2.5	14 ± 21	85 ± 23	0.0 ± 0.0	0.01 ± 0.01
Active floodplain	4	1.8 ± 0.5	45 ± 13	39 ± 20	5.5 ± 6.4	0.50 ± 0.17
Terrace	2	2.0 ± 0.0	13 ± 11	23 ± 18	14 ± 1.4	3.10 ± 0.46
Stable slope	4	22 ± 7.3	23 ± 24	28 ± 18	31 ± 9.0	3.11 ± 0.77
LGM moraine *	9	10 ± 10	27 ± 16	21 ± 8.2	21 ± 6.8	2.88 ± 1.48
Pre-LGM moraine	2	20 ± 7.1	18 ± 3.5	15 ± 0.0	36 ± 15	6.87 ± 0.31
Wetland	6	4.3 ± 3.1	1.3 ± 1.9	1.8 ± 1.7	63 ± 28	23.7 ± 15.0

* This class includes site T1-4 (see Table 2 footnote).

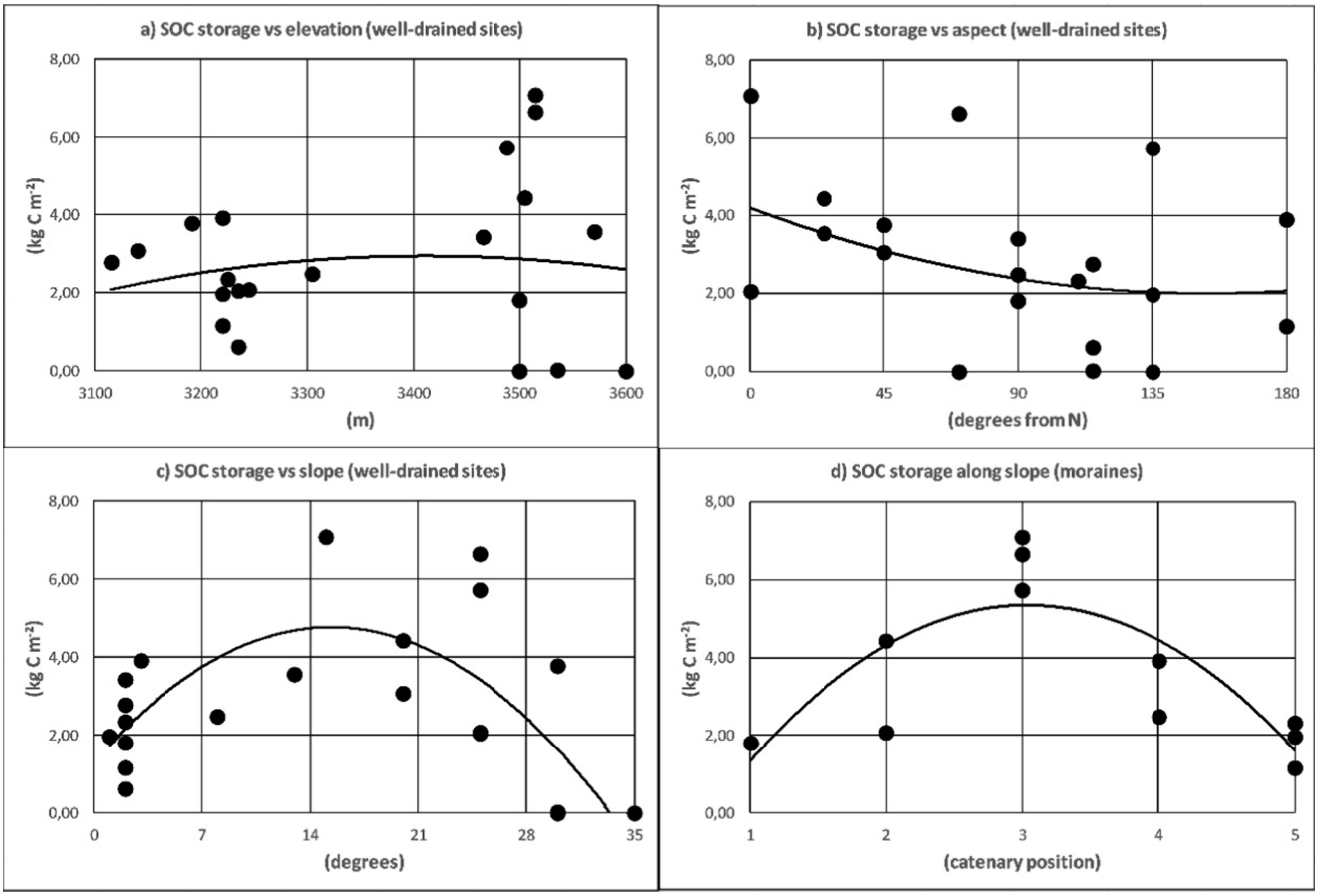

Fig. 6. Topographic controls on SOC storage (kg C m^{-2}) at well-drained sites in the Veguitas catchment (active floodplains and wetlands excluded). 2nd order polynomial regressions of SOC storage vs a) elevation ($p > 0.05$), b) aspect ($p > 0.05$), c) slope ($p < 0.05$) and d) catenary position on moraines 1 = crest, 2 = shoulder, 3 = backslope, 4 = footslope, 5 = hummocky ablation till ($p < 0.05$).

of meadow, shrub and sparse plant cover accounts for only 8.2% of the total study area. At low elevations, the snow-ice-water class corresponds to streams. The bare class has been subdivided in areas below 3900 m, where some minor vascular plant cover is still recognized, and the completely barren areas at higher elevations.

The meadow class is the C hotspot in the study area. SOC storage in the top 30 cm of soil is very narrowly constrained to c. 10–13 kg C m^{-2}, but more variable for the full depth of the deposit (12–53 kg C m^{-2}). Meadow site T1-10 is the only profile with additional C storage below 100 cm depth (49.04 kg C m^{-2} for 0–100 cm and 53.07 kg C m^{-2} for its full depth to 112 cm). The contribution of the meadow class to SOC 0–100 cm storage in the study area is low (<10%) because it accounts for only 0.11% of the total surface area of the Veguitas catchment and only 1.4% of its vegetated area.

The differences in SOC 0–100 cm storage between the shrub and sparse classes is small (4.1 and 3.1 kg C m^{-2}, respectively). Furthermore, c. 93–98% of the C stocks are found in the top 30 cm of these generally shallow soil profiles. While the separation of the shrub and sparse classes makes sense from a vegetation point of view (shrub class generally restricted to lower slopes), an amalgamation of the two classes for C stock calculations would have negligible impact, since profile replication in the classes closely reflect their proportional representation in the

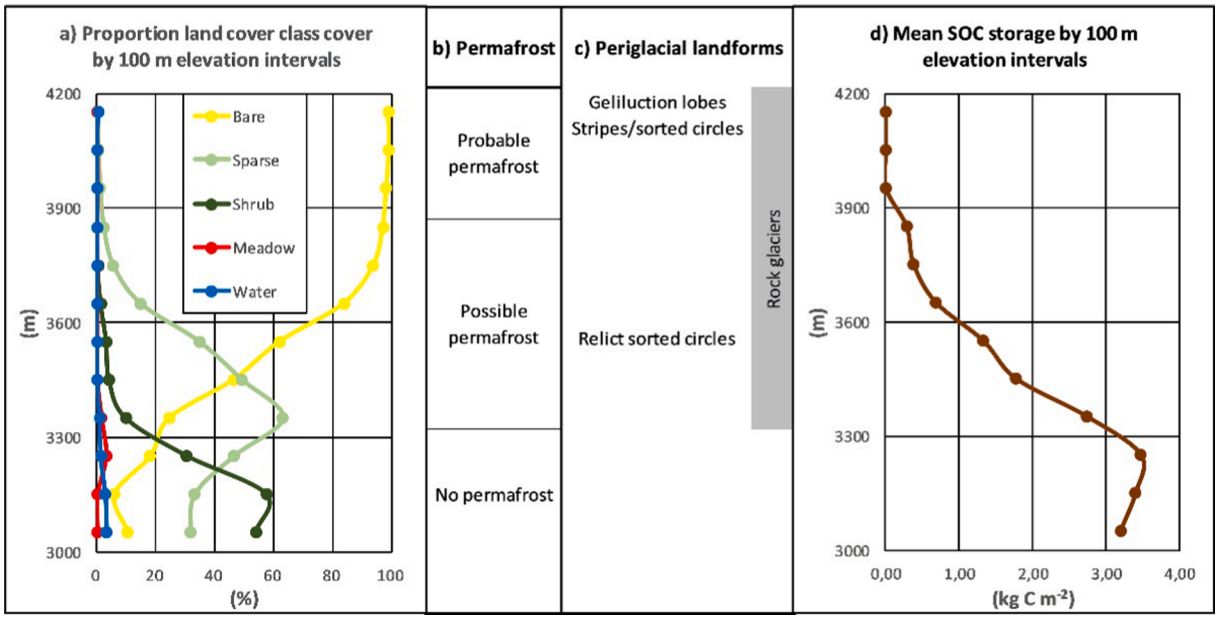

Fig. 7. a) Percent coverage of land cover classes by 100 m elevation intervals, b) mountain permafrost zones, c) observed periglacial features and d) weighed mean SOC 0–100 cm storage (kg C m^{-2}) by 100 m elevation intervals, in the lower portion of the Veguitas catchment (3000–4200 m) under current climatic conditions. (For interpretation of the references to color in this figure legend, the reader is referred to the web version of this article.)

study area.

The bare class < 3900 m elevation mostly includes active floodplains and active talus slopes without vegetation cover or SOC storage (0 kg C m^{-2}). Low terraces in floodplains and stable patches on steep slopes might harbor some plant cover and very low SOC stocks (0.02 to 0.67 kg C m^{-2}). Above 3900 m, we did not observe vascular plant cover or soil development (0 kg C m^{-2}).

Weighed mean SOC 0–100 cm storage is 0.33 kg C m^{-2} for the Veguitas catchment as a whole and 3.62 kg C m^{-2} for its vegetated area only. Confidence intervals are narrow due to reasonable profile replication per vegetated class, low standard deviations in the shrub and sparse classes, and low proportional area of the meadow class.

We also computed mean total SOC storage of our soil profiles, grouped into eight landform types (Table 3). Active slopes and floodplains have low SOC storage (<1 kg C m^{-2}). Stable surfaces on terraces (high floodplain terrace and kame terrace), on LGM moraines and on mountain slopes have SOC storages of 2.9–3.1 kg C m^{-2}. Pre-LGM moraine soils have the highest SOC storage for well-drained sites (6.9 kg C m^{-2}). The wetland class is identical to the meadow class in the land cover classification and has a mean total SOC storage of 23.7 kg C m^{-2}. These values apply to our soil profiles that were all collected in the elevation range of 3000–3600 m, below the vegetation limit in the study area. This approach has limited value to calculate a weighed, mean SOC storage for the entire study area because similar landforms (except wetlands) are recognized above the vegetation limit and hold no SOC stocks. Without adding vegetation criteria to the proportional representation of these landform types in the study area, no proper upscaling is feasible.

4.4. Topographic controls

We have analyzed the relationship between elevation, aspect and slope on SOC storage at our sites, using the complete dataset of collected soil profiles (n = 31) and only well-drained sites (n = 21). For the latter, we have excluded active floodplains and meadows (n = 10). In addition, we have assessed SOC storage on moraines (n = 11) using five catenary positions: crest, shoulder, backslope, footslope and hummocky ablation till. The latter category corresponds to gentle hummocks formed in ablation till (slopes < 3°).

Within the sampled range of 3000–3600 m, SOC storage in our soil profiles shows no significant trends with elevation. This holds for the complete dataset (R^2 = 0.04) as well as well-drained sites (Fig. 6a). Aspect shows no trend for the dataset as a whole (R^2 = 0.02), and a weak but non-significant trend towards higher SOC storage in well-drained sites with a more northern aspect (Fig. 6b). There is no significant relationship of SOC storage with slope for the full dataset (R^2 = 0.13), but a clear one if we consider well-drained sites only (Fig. 6c). Sites with slopes between 15 and 25° tend to have higher SOC stocks. Highest SOC storage on moraines is found in the backslope position (Fig. 6d). Two of the three backslope sites correspond to the pre-LGM moraine.

The SOC storage of single soil profiles show no trend with elevation (Fig. 6a). However, when we assign these sites to land cover classes and weigh their average SOC storage (Table 2) with the proportional representation of each land cover class at 100 m interval steps (Fig. 7a), a clear relationship emerges of decreasing SOC stocks with increasing elevation (Fig. 7d). Relatively high mean SOC storage (3–4 kg C m^{-2}) is found for the study area below 3300 m. Here, we find the SOC-rich meadow areas, as well as high coverage of the shrub class. Highest proportional coverage of the sparse class is found between 3200 and 3500 m, above which it gradually decreases whereas the bare class becomes more prominent with increasing elevation. At the same time, mean SOC storage decreases from c. 3 to < 0.5 kg C m^{-2} above the sparse vegetation limit at c. 3650 m. Higher up, vegetation is restricted to very small patches or single individuals up to 3900 m, with no observed vascular plant cover or soil development above this elevation. SOC storage is inferred to be small to negligible.

There is barely an overlap between plant cover and SOC storage with the inferred probable mountain permafrost zone (*in situ* aggraded) above the zero annual air isotherm at c. 3800–3900 m (Fig. 7b) or with active surface periglacial features observed at c. 4150 m (Fig. 7c). Permafrost at lower elevations is only encountered under rock glaciers, where the special insulation properties of the coarse rock debris preserves the underlying (creeping) permafrost body. In our study area, the lowest elevation of permafrost coincides with the terminus of the Stepanek rock glacier at c. 3350 m. Here, active rock glacier flow has precluded vegetation establishment and soil development. The only SOC stocks encountered on permafrost terrain correspond to an area with gentle slopes and stable surfaces on the inactive part of the Franke rock glacier between c. 3450–3650 m. This area of c. 0.05 km^2 (0.2% of the total study area) holds an estimated 3.56 kg C m^{-2} (soil profile T3-11) and represents 2.0% of the total SOC storage in the study area. The active layer in this type of permafrost setting is very deep and as a consequence no SOC stocks can be expected within the permafrost layer. Active degradation of permafrost at the Franke rock glacier edge creates steep, unstable slopes with negligible plant cover, soil development and SOC stocks (soil profile T3-10).

5. Discussion

There are significant relationships between soil depth, plant cover and SOC storage in the full Veguitas dataset. Soil depth explains 69% of plant cover and 94% of total SOC storage variability; plant cover explains 86% of observed variability in SOC 0–30 cm and 60% in SOC 0–100 cm storage. Greater soil depth provides a better substrate for plant establishment (below the vegetation limit). It also increases the volume of soil matrix that can hold SOC stocks. Plant cover provides the litter input for SOC accretion. Areas above the vegetation limit at c. 3650 m are all but devoid of plant cover and display no soil development (even on stable surfaces with fine-grained ground textures). At lower elevations, active (talus) slopes, active floodplains and active rock glaciers have no plant cover and no SOC stocks.

The vegetated area represents only 8.2% of the total Veguitas catchment. The vast majority of this area (98.6%) is occupied by sparse and shrub plant cover on well-drained sites. These areas have shallow soil profiles (average 23 and 27 cm, respectively) and low SOC stocks (average 3.1 and 4.1 kg C m^{-2}, respectively). SOC is largely confined to the top 30 cm of soil profiles (98 and 93%, respectively), which is typical for this type of mountain setting (Bockheim and Munroe, 2014). Highest SOC storage in well-drained sites is found on the pre-LGM moraine (average 6.9 kg C m^{-2}). Radiocarbon dates on a B-horizon and a deep woody root remain in one of these pre-LGM moraine sites are very young (501 cal yr BP) and 'modern' in age, suggesting rapid SOC cycling. Wayne and Corte (1983) described soils on the pre-LGM moraines as Mollisols with a weakly developed B-horizon. A soil developed into the high terrace of a glacio-fluvial floodplain at c. 3500 m is also interpreted to be recent age (site T3-3). The formation of the now relict sorted circles at this site can be tentatively assigned to the Little Ice Age (Espizua and Pitte, 2009), with vegetation establishment, soil development and SOC accretion likely postdating the end of this cold period around 1900AD. Dated root material at various depths in this site are 'modern' in age, supporting a young age of soil formation.

The wet meadow sites have a very dense cover of graminoids and much deeper soil profiles (average 63 cm). They are hotspots of SOC storage (average 23.7 kg C m^{-2}), but contribute little to overall stocks in the Veguitas catchment due to their very limited extent (0.11% of total study area and 1.4% of the vegetated area). Some meadow sites can be considered Histosols (>40 cm peat), other Histic Gleysols. Despite their high SOC storage, three dated sites have relatively young basal dates (<1100 cal yr BP). Net C accumulation rates are consequently high, particularly in recent times (37–82 gC m^{-2} yr^{-1}). Young basal ages and high recent accumulation rates have also been reported from high mountain meadows ('bofedales') in the dry Chilean Andes (Earle et al., 2003). In our study, meadows are found on relatively flat areas supplied by water discharge from a nearby rock glacier (Franke meadow) and from an up-valley glacier and rock glacier area (Veguitas meadows). Recent vegetation and surface hydrology dynamics of the Franke and Veguitas meadow areas over the period 2002–2019, tracked using remotely sensed NDVI and NDWI variations, are described in Pecker and Trombotto (2021).

The Franke meadow T1-10 site with the deepest peat deposit (102 cm) in the Veguitas catchment has interesting stratigraphy and chronology, although the usual uncertainties associated with radiocarbon dating in subrecent times makes an unambiguous age-depth model unattainable. Two layers with increased minerogenic input in this peat sequence seem to correspond to an early and late phase of the Little Ice Age (centered around c. 1650AD and 1850AD). These periods are characterized by glacier advances in the nearby Peteroa Volcano region (Espizua and Pitte, 2009), and might have triggered locally an activation of slope processes in the direct surroundings of the Franke meadow. Alternatively, warming at the end of these cold phases could have triggered slope instability due to permafrost thaw as well as increased water discharge and sediment supply from the degrading Franke rock glacier terminus.

Only 2% of SOC stocks in the Veguitas catchment is located in permafrost terrain, i.e. the stable surfaces with gentle slopes of the inactive part of the Franke rock glacier located below the vegetation limit (<3650 m). As is the case at all other well-drained, vegetated sites in the study area, c. 95% of the total SOC (3.56 kg C m^{-2}) was located in the top 30 cm of a 37 cm deep soil profile (site T3-11). No SOC can be expected in the permafrost layer at these rock glacier sites, characterized by deep active layers (Trombotto and Borzotta, 2009). Site T3-10 on the steep, degrading edge of the Franke rock glacier terminus had very sparse plant cover and negligible SOC stocks (0.02 kg C m^{-2}). The lower part of the Stepanek rock glacier is active and characterized by a typical lobate structure associated with permafrost creep. Its surface has no plant cover or soil development, even below the vegetation limit in the study area (<3650 m). Furthermore, we did not observe any plant cover or soil development in other areas with active periglacial activity (gelifluction, patterned ground), which were restricted to elevations of > 4100 m.

The Veguitas catchment (3000–5500 m) has a mean SOC 0–100 cm storage of 0.3 kg C m^{-2} (3.6 kg C m^{-2} for vegetated area only), which is comparable to values reported for other investigated mountain permafrost areas. Fuchs et al. (2015) reported that the high-alpine Tarfala valley (500–2100 m), in the Scandes Mountains of northern Sweden, has a mean SOC 0–100 cm storage of 0.9 kg C m^{-2} for total study area and 4.6 kg C m^{-2} for vegetated area only. In both these areas there is very limited overlap between the upper vegetation belt and the mountain permafrost zone. As a consequence, negligible amounts of SOC are stored in permafrost. Detailed SOC inventories have also been conducted in high-alpine and high-arctic mountain settings located in continuous permafrost terrain. The upper reaches of Aktru valley (2100–4000 m), in the High Altai of Central Asia, has a mean SOC 0–100 cm storage of 0.9 kg C m^{-2} for total study area and 3.1 kg C m^{-2} for vegetated area only (adapted from Pascual et al., 2020). Wojcik et al. (2019) give values of 1.0 kg C m^{-2} for total study area and 4.2 kg C m^{-2} for vegetated area only for a high-arctic mountainous area on Brøgger Peninsula (0–900 m), Svalbard. Even though both the Aktru and Brøgger areas are located in continuous permafrost terrain, negligible amounts of SOC are stored in the permafrost layer due to deep active layers characteristic of mountain settings (Bockheim and Munroe, 2014). All four study areas have in common that mean SOC storage is significantly reduced due to the high proportion of bare ground areas. The vegetated areas account for only 8% (Veguitas), 27% (Tarfala), 19% (Aktru) and 18% (Brøgger) of the total study areas.

The additional studies mentioned above were carried out using similar fieldwork and upscaling approaches, taken great care in acknowledging the negligible contribution to mean SOC storage of

extensive bare ground areas typical of mountain settings. They have further in common that they are all located within the contiguous northern permafrost region in the domain of the Northern Circumpolar Soil Carbon Database, or NCSCD (Tarnocai et al., 2009; Hugelius et al., 2014; NCSCDv2, 2014). The review by Bockheim and Munroe (2014) on soils in the global mountain permafrost area includes data on SOC storage in vegetated areas of mountain ranges not considered in the NCSCD. Due to similar climatic conditions and altitudinal ranges, the arid/semiarid area of the Tibetan Plateau is of greatest interest for a comparison with the Veguitas dataset although the former includes plateau areas with deep unconsolidated deposits that hold significant SOC stocks at > 1 m depth (Mu et al., 2015; Ding et al., 2016). Wang et al. (2002) report for shallow profiles in the Qinghai-Tibetan Plateau mean SOC values of 1.5–4.1 kg C m^{-2} under alpine (cold) desert (mean soil depth 22–45 cm), 9.0–16.2 kg C m^{-2} for alpine steppe (mean soil depth 60 cm) and 10.9–53.1 kg C m^{-2} for different types of meadow (mean soil depth 50–110 cm). Ohtsuka et al. (2008) investigated plant cover and SOC 0–30 cm storage along an altitudinal gradient between 4400 and 5300 m in the Nyainqentanglha Mountains of southern Tibet. Plant cover and SOC storage ranged between 13.3-88.3% and 2.6–13.7 kg C m^{-2} below the alpine vegetation limit, but were greatly reduced to < 1% and 1.0 kg C m^{-2} at the highest elevation site in the nival zone.

Even though locally peat deposits and high plateau sediments can increase SOC stocks, mountain permafrost settings generally have about an order of magnitude lower mean SOC 0–100 cm storage compared to lowland areas across the northern circumpolar permafrost region, where values can range between c. 15 and 40 kg C m^{-2} of which 25–67% is located in the permafrost layer (e.g., Hugelius et al., 2010; Siewert et al., 2015; Palmtag et al., 2016). Furthermore, lowland permafrost areas often have significant SOC stocks below 100 cm in deep cryoturbated soils and peat deposits that are typically rare in mountain permafrost settings. In northern lowlands, the gradual and abrupt thaw of permafrost SOC stocks under conditions of enhanced global warming (polar amplification) is projected to result in large releases of greenhouse gases to the atmosphere (Schuur et al., 2015; Turetsky et al., 2020). These losses are expected to exceed any gains from increased phytomass C uptake as tundra is replaced by forest (Abbott et al., 2016). The region is expected to become a net C source, representing a positive feedback on global warming.

The effects of global warming on C stocks in mountain settings can be very different. The Central Andes are projected to warm approximately at the global average, i.e. c. 1 °C under RCP2.6 and 3.5 °C under RCP8.5 (Representative Concentration Pathways) by the end of this Century, with limited changes in precipitation (Magrin et al., 2014), even if the consequences of an Elevation-Dependent-Warming remain uncertain (Pepin et al., 2015). With an approximate thermal lapse rate of 0.6 °C / 100 m, the RCP8.5 scenario could imply an upward shift in ecoclimatic zones of c. 600 m. The potential vegetation limit with soil development could migrate to c. 4200 m, with new C sequestration in phytomass and soils at favorable locations (e.g., on stable mountain slopes, moraines, high terraces of floodplains, etc.). Tall *Adesmia* shrub communities could replace more open vegetation stands at mid-elevation, whereas sparse vegetation could occupy currently bare ground areas at high elevation. These changes would represent an approximate increase in phytomass C of 0.5 to 1.5 kg C m^{-2}. At the same time, total SOC storage at newly vegetated sites could increase by 3–4 kg C m^{-2} (and more, if new wetlands are established in areas with summer water supply from glaciers and rock glaciers). Future permafrost degradation cannot cause losses since no SOC was encountered in the current permafrost layer. Indirectly, slope destabilization and rock glacier degradation due to permafrost thaw could locally affect current phytomass and soil C stocks or prevent vegetation establishment and soil development in the future. Notwithstanding, the Veguitas catchment as a whole will see an increase in vegetated area with soil development and associated phytomass and soil C stocks. This type of high mountain periglacial environment is thus likely to represent a negative feedback on global warming (see also Fuchs et al., 2015; Wojcik et al., 2019; Pascual et al., 2020). The strength of this new C sink will depend on the rate of upward vegetation establishment and soil development. A full analysis of the role of the global mountain permafrost area in the permafrost C feedback is still pending. Furthermore, any C gains at high elevations have to be compared to climate effects on total ecosystem C storage in the mountain vegetation belts downslope.

6. Conclusions

No previous SOC inventories have been conducted in the mountain permafrost zone of the semi-arid Central Andes. Our results for the Veguitas catchment show that this type of high mountain environment hold very low SOC stocks, when properly considering the large proportion of snow and ice-covered terrain, extensive bare ground at high elevation and even below the upper vegetation limit on active surfaces like steep (talus) slopes, active floodplains and active rock glaciers. Mean SOC 0–100 cm storage in the Veguitas catchment (3000–5500 m) is only 0.33 kg C m^{-2} when considering the full study area, and 3.62 kg C m^{-2} when considering the 8.2% vegetated area in the catchment below the vegetation limit at c. 3650 m. Our analyses further show that there is very limited overlap between the upper vegetation belt with soil development and the mountain permafrost zone. The current elevation of the mean annual zero isotherm is estimated to be located at c. 3800–3900 m, with extensive mountain permafrost only probable above these elevations. The only overlap between vegetated area with soil development and permafrost was on the inactive part of a rock glacier between c. 3450–3650 m. Here, SOC 0–100 cm storage in one profile was 3.56 kg C m^{-2} close to the mean for the vegetated area of the Veguitas catchment. However, none of this stock is located within the permafrost layer itself because of deep active layers in the coarse debris typical for rock glaciers. Future global warming will thus not remobilize any currently frozen SOC stocks leading to C releases to the atmosphere. On the contrary, an upward shift of the upper vegetation belt with soil development will create new areas of phytomass and soil C storage that only locally might be constrained by permafrost thaw leading to slope destabilization and rock glacier degradation. The Veguitas catchment will most likely represent a future net C sink in a warming climate.

Declaration of Competing Interest

The authors declare that they have no known competing financial interests or personal relationships that could have appeared to influence the work reported in this paper.

Acknowledgments

We would like to thank Ms. Sandra Viviana Muñoz (Refugio San Bernardo) for her hospitality and support during the fieldtrip. Fieldwork and analyses were supported by the European Union (EU) Joint Programming Initiative (JPI) on Climate ‘Constraining Uncertainties in the Permafrost–Climate Feedback (COUP)’ consortium.

Appendix

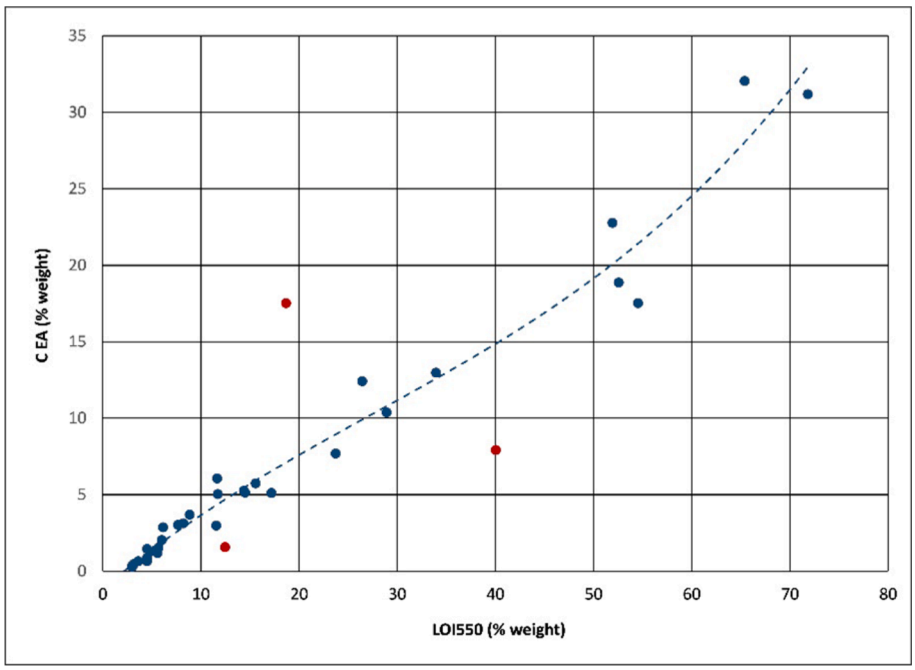

Fig. A1. 3rd order polynomial regression between %LOI at 550 °C and %C from Elemental Analysis. Three outliers are excluded from the regression (red dots). (For interpretation of the references to color in this figure legend, the reader is referred to the web version of this article.)

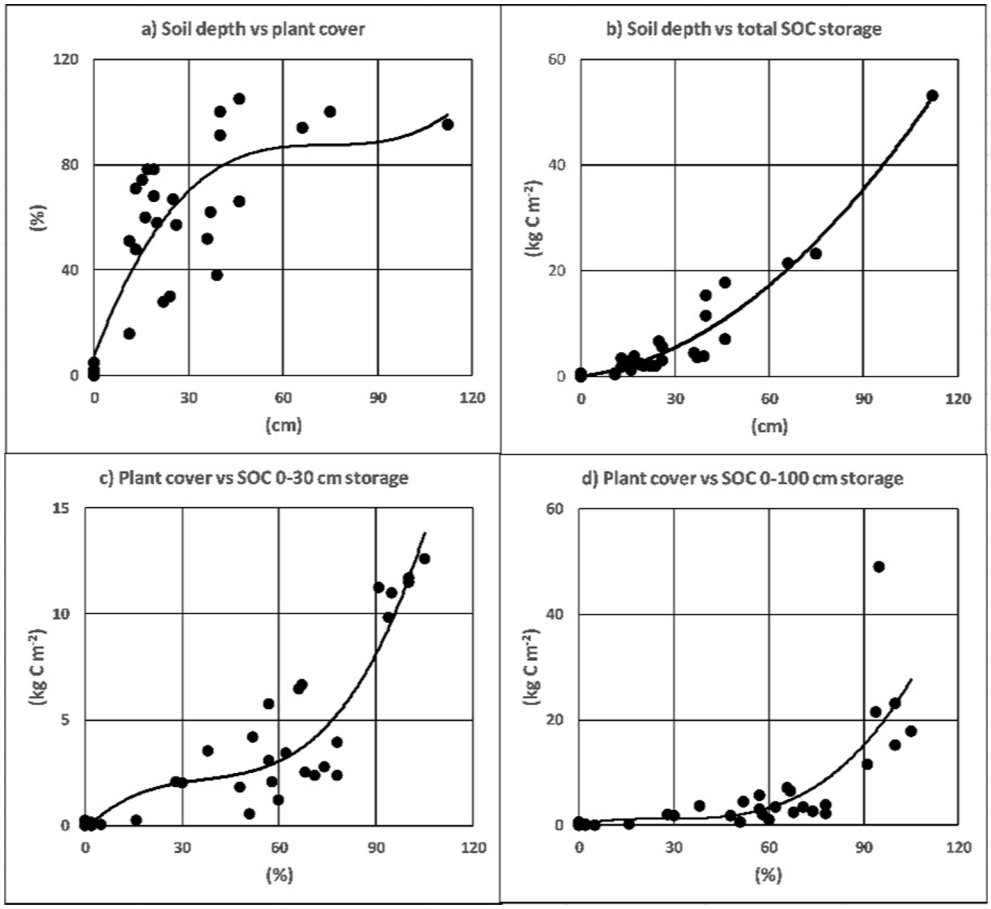

Fig. A2. 3rd order polynomial regressions of a) Soil depth vs plant cover, b) Soil depth vs total SOC storage, c) Plant cover vs SOC 0–30 cm and d) Plant cover vs SOC 0–100 cm storage, for all sampled soil profiles.

Table A1
Transect and soil profile summary with geographic coordinates, topography (altitude, slope and aspect), catenary position (na = not applicable), landform type, surface cover of bare mineral ground (grain size < 4 cm) and large stones (grain size ≥ 4 cm), and soil profile depth . * Geographic coordinates for profile sites T3-1 and T3-12 are approximate because exact location could not be reached due to rock avalanche risk.

Transect/ Profile	South latitude	West longitude	Elevation (m)	Slope (degrees)	Aspect 1 (degrees)	Aspect 2 (degrees from North)	Catena class code	Catena class name	Landform type	Bare ground (% cover)	Large stones (% cover)	Profile depth (cm)
LV T1-1	32° 58.511′	69° 21.968′	3115	2	115	115	5	Flat	Kame terrace	5	35	15
LV T1-2	32° 58.524′	69° 22.031′	3140	20	45	45	3	Backslope	Stable slope	10	35	26
LV T1-3	32° 58.536′	69° 22.094′	3192	30	45	45	3	Backslope	Stable slope	55	10	39
LV T1-4	32° 58.547′	69° 22.156′	3220	3	180	180	4	Footslope	LGM moraine	10	15	17
LV T1-5	32° 58.558′	69° 22.217′	3225	2	70	70	na	na	Wetland	1	2	66
LV T1-6	32° 58.575′	69° 22.285′	3225	2	250	110	5	Hummocky	LGM moraine	10	20	19
LV T1-7	32° 58.585′	69° 22.347′	3235	2	115	115	5	Flat	Floodpl low terrace	40	10	11
LV T1-8	32° 58.597′	69° 22.408′	3235	1	115	115	na	na	Active floodplain	60	40	0
LV T1-9	32° 58.608′	69° 22.473′	3262	8	90	90	na	na	Wetland	0	0	75
LV T1-10	32° 58.619′	69° 22.536′	3275	8	70	70	na	na	Wetland	0	5	112
LV T1-11	32° 58.631′	69° 22.597′	3305	8	90	90	4	Footslope	LGM moraine	30	15	19
LV T2-1	32° 58.678′	69° 22.285′	3235	25	0/360	0	3	Backslope	Stable slope	1	50	20
LV T2-2	32° 58.642′	69° 22.270′	3220	2	90	90	na	na	Active floodplain	30	55	11
LV T2-3	32° 58.599′	69° 22.257′	3220	1	225	135	5	Hummocky	LGM moraine	60	15	24
LV T2-4	32° 58.571′	69° 22.248′	3220	2	180	180	5	Hummocky	LGM moraine	25	15	16
LV T2-5	32° 58.546′	69° 22.238′	3228	1	115	115	na	na	Wetland	1	2	46
LV T2-6	32° 58.525′	69° 22.228′	3230	2	135	135	na	na	Wetland	5	1	40
LV T2-7	32° 58.498′	69° 22.224′	3235	5	180	180	na	na	Wetland	1	1	40
LV T2-8	32° 58.475′	69° 22.208′	3245	25	0/360	0	2	Shoulder	LGM moraine	40	25	22
LV T3-1*	32° 58.500′	69° 23.137′	3500	35	135	135	3	Backslope	Active talus	0	100	0
LV T3-2	32° 58.545′	69° 23.100′	3500	2	90	90	1	Crest	LGM moraine	30	25	13
LV T3-3	32° 58.586′	69° 23.065′	3465	2	90	90	5	Flat	Floodpl high terrace	20	10	13
LV T3-4	32° 58.631′	69° 23.028′	3470	2	70	70	na	na	Active floodplain	49	50	0
LV T3-5	32° 58.675′	69° 22.989′	3488	25	135	135	3	Backslope	LGM moraine	25	20	26
LV T3-6	32° 58.720′	69° 22.951′	3505	20	335	25	2	Shoulder	LGM moraine	10	40	36
LV T3-7	32° 58.762′	69° 22.914′	3515	15	0/360	0	3	Backslope	Pre-LGM moraine	20	15	46
LV T3-8	32° 58.809′	69° 22.878′	3515	25	70	70	3	Backslope	Pre-LGM moraine	15	15	25
LV T3-9	32° 58.852′	69° 22.840′	3500	30	70	70	3	Backslope	Active talus	5	95	0
LV T3-10	32° 58.896′	69° 22.805′	3535	30	115	115	3	Backslope	Rock gl (degrading)	45	50	0
LV T3-11	32° 58.941′	69° 22.769′	3570	13	25	25	3	Backslope	Rock gl (stable slope)	25	15	37
LV T3-12*	32° 58.986′	69° 22.732′	3600	30	225	135	3	Backslope	Active talus	5	95	0

(*continued on next page*)

Table A1 (*continued*)

Transect and soil profile summary with land cover class, mean height of upper vegetation stratum, cover of plant functional types, litter and sum of surface mineral (bare ground and large stones).

Transect/ Profile	Elevation (m)	Land cover class name	Height Vegetation (cm)	Shrub ≥25cm (% cover)	Dwarfshrub <25cm (% cover)	Grass (% cover)	Cushion (% cover)	Wetland Graminoid (% cover)	Forb (% cover)	Moss (% cover)	Lichen (% cover)	Litter (% cover)	Surface mineral (% cover)

Transect and soil profile summary with land cover class, mean height of upper vegetation stratum, cover of plant functional types, litter and sum of surface mineral (bare ground and large stones).

Transect/ Profile	Elevation (m)	Land cover class name	Height Vegetation (cm)	Shrub ≥25cm (% cover)	Dwarfshrub <25cm (% cover)	Grass (% cover)	Cushion (% cover)	Wetland Graminoid (% cover)	Forb (% cover)	Moss (% cover)	Lichen (% cover)	Litter (% cover)	Surface mineral (% cover)
LV T1-1	3115	Sparse	15	0	2	20	25	0	2	0	10	15	40
LV T1-2	3140	Shrub	25	1	14	20	5	0	1	1	5	10	45
LV T1-3	3192	Sparse	25	5	5	20	0	0	2	0	1	5	65
LV T1-4	3220	Sparse	5	0	0	10	60	0	1	0	2	5	25
LV T1-5	3225	Meadow	2	0	0	0	0	85	1	3	0	5	3
LV T1-6	3225	Sparse	15	0	5	10	50	0	5	0	3	5	30
LV T1-7	3235	Sparse	10	0	5	10	25	0	3	0	3	5	50
LV T1-8	3235	Bare	0	0	0	0	0	0	0	0	0	0	100
LV T1-9	3262	Meadow	2	0	0	0	0	100	0	0	0	0	0
LV T1-10	3275	Meadow	5	0	0	0	0	90	0	0	0	5	5
LV T1-11	3305	Sparse	15	0	15	20	10	0	10	0	3	10	45
LV T2-1	3235	Shrub	100	20	10	20	0	0	2	0	1	5	51
LV T2-2	3220	Bare	70	1	10	2	0	0	1	0	2	0	85
LV T2-3	3220	Sparse	5	0	0	20	5	0	1	0	2	2	75
LV T2-4	3220	Sparse	5	0	1	20	30	0	3	0	1	5	40
LV T2-5	3228	Meadow	2	0	0	0	0	90	5	5	5	0	3
LV T2-6	3230	Meadow	2	0	0	0	5	70	0	20	0	5	6
LV T2-7	3235	Meadow	2	0	0	0	0	85	1	2	0	3	2
LV T2-8	3245	Sparse	100	3	5	15	0	0	3	0	1	1	65
LV T3-1	3500	Bare	0	0	0	0	0	0	0	0	0	0	100
LV T3-2	3500	Sparse	8	0	1	10	20	0	1	0	1	15	55
LV T3-3	3465	Sparse	5	0	0	15	40	0	5	0	1	10	30
LV T3-4	3470	Bare	5	0	0	1	0	0	0	1	0	0	99
LV T3-5	3488	Sparse	5	0	0	25	15	0	10	0	2	5	45
LV T3-6	3505	Shrub	15	0	5	15	25	0	2	0	3	2	50
LV T3-7	3515	Sparse	15	0	10	15	35	0	1	0	2	3	35
LV T3-8	3515	Shrub	15	0	10	20	25	0	1	0	1	10	30
LV T3-9	3500	Bare	2	0	0	0	0	0	1	0	1	0	100
LV T3-10	3535	Bare	25	3	0	1	0	0	1	0	0	0	95
LV T3-11	3570	Sparse	15	0	15	15	20	0	1	0	1	10	40
LV T3-12	3600	Bare	0	0	0	0	0	0	0	0	0	0	100

References

Abbott, B.W., Jones, J.B., Schuur, E.A.G., et al., 2016. Biomass offsets little or none of permafrost carbon release from soils, streams, and wildfire: An expert assessment. Environ. Res. Lett. 11 (3), 034014 https://doi.org/10.1088/1748-9326/11/3/034014.

Barros, A., Pickering, C.M., Renison, D., 2014. Short-Term Effects of Pack Animal Grazing Exclusion from Andean Alpine Meadows. Arct. Antarct. Alp. Res. 46, 333–343. https://doi.org/10.1657/1938-4246-46.2.333.

Bockheim, J.G., Munroe, J.S., 2014. Organic carbon pools and genesis of alpine soils with permafrost: A review. Arct. Antarct. Alp. Res. 46, 987–1006. https://doi.org/10.1657/1938-4246-46.4.987.

Bronk Ramsey, C., 2009. Bayesian analysis of radiocarbon dates. Radiocarbon 51 (1), 337–360.

Campbell, J.B., Wynne, R.H., 2011. Introduction to remote sensing, 5th ed. Guilford Press, New York, p. 662.

Ding, J., Li, F., Yang, G., Chen, L., Zhang, B., Liu, L., Fang, K., Qin, S., Chen, Y., Peng, Y., Ji, C., He, H., Smith, P., Yang, Y., 2016. The permafrost carbon inventory on the Tibetan Plateau: a new evaluation using deep sediment cores. Glob. Change Biol. 22, 2688–2701. https://doi.org/10.1111/gcb.13257.

Earle, L.R., Warner, B.G., Aravena, R., 2003. Rapid development of an unusual peat-accumulating ecosystem in the Chilean Altiplano. Quaternary Res. 59, 2–11. https://doi.org/10.1016/S0033-5894(02)00011-X.

Espizua, L.E., Pitte, P., 2009. The Little Ice Age glacier advance in the Central Andes (35°S), Argentina. Palaeogeog., Palaeoclim Palaeoecol. 281, 345–350. https://doi.org/10.1016/j.palaeo.2008.10.032.

Fuchs, M., Kuhry, P., Hugelius, G., 2015. Low below-ground organic carbon storage in a subarctic Alpine permafrost environment. Cryosphere 9, 427–438. https://doi.org/10.5194/tc-9-427-2015.

Gorbunov, A.P., 1978. Permafrost investigation in high mountain regions. Arct. Alp. Res 10, 283–294. https://doi.org/10.1080/00040851.1978.12003967.

Gruber, N., Friedlingstein, P., Field, C.B., Valentini, R., Heimann, M., Richey, J.E., Romero-Lankao, P., Schulze, D., Chen, C.-T. A., 2004. The vulnerability of the carbon cycle in the 21st century: An assessment of carbon-climate-human interactions, in: The Global Carbon Cycle, Integrating Humans, Climate and the Natural World, edited by: Field, C. and Raupach, M., Island Press, Washington DC, 45-76.

Haeberli, W., Guodong, C., Gorbunov, A., Harris, S., 1993. Mountain Permafrost and Climatic Change. Permafr. Periglac. Process. 4, 165–174. https://doi.org/10.1002/ppp.3430040208.

Hammer, Ø., Harper, D.A.T., Ryan, P.D., 2001. PAST: Paleontological Statistics Software Package for Education and Data Analysis. Palaeontol. Electron. 4, 9 pp.

Heiri, O., Lotter, A.F., Lemcke, G., 2001. Loss on ignition as a method for estimating organic and carbonate content in sediments: Reproducibility comparability of results. J. Paleolimnol. 25, 101–110. https://doi.org/10.1023/A:1008119611481.

Hoffmann, A.J., 1982. Altitudinal ranges of phanerophytes and chamaephytes in central Chile. Vegetatio 48 (2), 151–163.

Hogg, A.G., Heaton, T.J., Hua, Q., Palmer, J.G., Turney, C.SM., Southon, J., Bayliss, A., Blackwell, P.G., Boswijk, G., Bronk Ramsey, C., Pearson, C., Petchey, F., Reimer, P., Reimer, R., Wacker, L., 2020. SHCal20 Southern Hemisphere calibration, 0–55,000 years cal BP. Radiocarbon 62 (4), 759–778.

Hua, Q., Barbetti, M., Rakowski, A.J., 2013. Atmospheric Radiocarbon for the Period 1950–2010. Radiocarbon 55, 2059–2072. https://doi.org/10.2458/azu_js_rc.v55i2.16177.

Hugelius, G., Kuhry, P., Tarnocai, C., Virtanen, T., 2010. Soil organic carbon pools in a periglacial landscape: a case study from the central Canadian Arctic. Permafr. Periglac. Process. 21, 16–29. https://doi.org/10.1002/ppp.677.

Hugelius, G., 2012. Spatial upscaling using thematic maps: An analysis of uncertainties in permafrost soil carbon estimates. Glob. Biogeochem. Cycles 26 (GB2026.). https://doi.org/10.1029/2011GB004154.

Hugelius, G., Strauss, J., Zubrzycki, S., Harden, J.W., Schuur, E.A.G., Ping, C.-L., Schirrmeister, L., Grosse, G., Michaelson, G.J., Koven, C.D., O'Donnell, J.A., Elberling, B., Mishra, U., Camill, P., Yu, Z., Palmtag, J., Kuhry, P., 2014. Estimated stocks of circumpolar permafrost carbon with quantified uncertainty ranges and identified data gaps. Biogeosciences 11, 6573–6593. https://doi.org/10.5194/bg-11-6573-2014.

IUSS Working Group WRB, 2006. World Reference Base for Soil Resources, 2006. World Soil Resources Reports, 103. FAO, Rome.

Jones, H.G., Vaughan, R.A., 2010. Remote sensing of vegetation. Oxford University Press 164–172.

Magrin, G.O., Marengo, J.A., Boulanger, J.-P., Buckeridge, M.S., Castellanos, E., Poveda, G., Scarano, F.R., Vicuña, S., 2014. Central and South America. In: Climate Change 2014: Impacts, Adaptation, and Vulnerability. Part B: Regional Aspects. Contribution of Working Group II to the Fifth Assessment Report of the Intergovernmental Panel on Climate Change [Barros, V.R., C.B. Field, D.J. Dokken, M.D. Mastrandrea, K.J. Mach, T.E. Bilir, M. Chatterjee, K.L. Ebi, Y.O. Estrada, R.C. Genova, B. Girma, E.S. Kissel, A.N. Levy, S. MacCracken, P.R. Mastrandrea, L.L.White (eds.)]. Cambridge University Press, Cambridge, United Kingdom and New York, NY, USA, pp. 1499-1566.

Méndez, E., 2004. La vegetación de los Altos Andes I. Pisos de vegetación del flanco oriental del Cordón del Plata, Mendoza Argentina. Bol. Soc. Argent. Bot. 39, 227–253.

Méndez, E., Martinez Carretero, E., Peralta, I., 2006. La vegetación del Parque Provincial Aconcagua (Altos Andes Centrales de Mendoza, Argentina). Bol. Soc. Argent. Bot. 41, 41–49.

Méndez, E., 2007. La vegetación de los Altos Andes II. Pisos de vegetación del flanco oriental Del Cordón del Plata (Mendoza, Argentina). Bol. Soc. Argent. Bot. 39, 227–253.

Mu, C., Zhang, T., Wu, Q., Peng, X., Cao, B., Zhang, X., Cao, B., Cheng, G., 2015. Organic carbon pools in permafrost regions on the Qinghai-Xizang (Tibetan) Plateau. Cryosphere 9, 479–486. https://doi.org/10.5194/tc-9-479-2015.

NCSCDv2, 2014. The Northern Circumpolar Soil Carbon Database, version 2. 10.5879/ECDS/00000002.

Ohtsuka, T., Hirota, M., Zhang, X., Shimono, A., Senga, Y., Du, M., Yonemura, S., Kawashima, S., Tang, Y., 2008. Soil organic carbon pools in alpine to nival zones along an altitudinal gradient (4400–5300 m) on the Tibetan Plateau. Polar Sci. 2, 277–285. https://doi.org/10.1016/j.polar.2008.08.003.

Oñatibia, G.R., Aguiar, M.R., Cipriotti, P.A., Troiano, F., 2010. Individual plant and population biomass of dominant shrubs in Patagonian grazed fields. Ecología Austr. 20, 269–279.

Palmtag, J., Ramage, J., Hugelius, G., Gentsch, N., Lashchinskiy, N., Richter, A., Kuhry, P., 2016. Controls on the storage of organic carbon in permafrost soil in northern Siberia. Eur. J. Soil Sci. 67, 478–491. https://doi.org/10.1111/ejss.12357.

Pascual, D., Kuhry, P., Raudina, T., 2021. Soil organic carbon storage in a mountain permafrost area of Central Asia (High Altai. Ambio 50 (11), 2022–2037.

Pecker Marcosig, I., Trombotto Liaudat, D., 2021. Análisis de la dinámica de dos mallines de altura en Vallecitos, Cordón del Plata, Mendoza, Argentina en el periodo 2002-2019. Acta Geológica Lilloana, 33(1), 1–24. 10.30550/j.agl/2021.33.1/2021-02-18.

Pepin, N., Bradley, R., Diaz, H.F., Baraer, M., Caceres, E.B., Forsythe, N., Fowler, H., Greenwood, G., Hashmi, M.Z., Liu, X.D., Miller, J.R., Ning, L., Ohmura, A., Palazzi, E., Rangwala, I., Schöner, W., Severskiy, I., Shahgedanova, M., Wang, M.B., Williamson, S.N., Yang, D.Q., 2015. Elevation-dependent warming in mountain regions of the world. Nat. Clim. Change 5, 424–430. https://doi.org/10.1038/nclimate2563.

Saito, K., Trombotto Liaudat, D., Yoshikawa, K., Mori, J., Sone, T., Marchenko, S., Romanovsky, V., Walsh, J., Hendricks, A., Bottegal, E., 2015. Late Quaternary permafrost distributions downscaled for South America: Examinations of GCM-based maps with observations. Permafr. Periglac. Process. 27, 43–55. https://doi.org/10.1002/ppp.1863.

Schuur, E.A.G., McGuire, A.D., Schädel, C., Grosse, G., Harden, J.W., Hayes, D.J., Hugelius, G., Koven, C.D., Kuhry, P., Lawrence, D.M., Natali, S.M., Olefeldt, D., Romanovsky, V.E., Schaefer, K., Turetsky, M.R., Treat, C.C., Vonk, J.E., 2015. Climate change and the permafrost carbon feedback. Nature 20, 171–179. https://doi.org/10.1038/nature14338.

Siewert, M.B., Hanisch, J., Weiss, N., Kuhry, P., Maximov, T.C., Hugelius, G., 2015. Comparing carbon storage of Siberian tundra and taiga permafrost ecosystems at very high spatial resolution. J. Geophys. Res. Biogeosci. 120, 1973–1994. https://doi.org/10.1002/2015JG002999.

Sileo, N.R., Dapeña, C., Trombotto Liaudat, D., 2020. Isotopic Composition and Hydrogeochemistry of a Periglacial Andean Catchment and its Relevance in the Knowledge of Water Resources in Mountainous Areas. Isotopes Environ. Health Stud. 56 (5-6), 480–494.

Soil Survey Staff, 2014. Keys to Soil Taxonomy, 12th Edition, USDA Natural Resources Conservation Service, Washington, D.C.

Tarnocai, C., Canadell, J.G., Schuur, E.A.G., Kuhry, P., Mazhitova, G., Zimov, S., 2009. Soil organic carbon pools in the northern circumpolar permafrost region. Glob. Biogeochem. Cycles 23 (GB2023). https://doi.org/10.1029/2008GB003327.

Thompson, S.K., 1992. Sampling. John Wiley, New York, p. 343.

Trombotto, D., Borzotta, E., 2009. Indicators of present global warming through changes in active-layer thickness, estimation of thermal diffusivity and geomorphological observations in the Morenas Coloradas rockglacier, central Andes of Mendoza. Argentina. Cold Reg. Sci. Technol. 55, 321–330. https://doi.org/10.1016/j.coldregions.2008.08.009.

Trombotto Liaudat, D., Sileo, N., Dapeña, C., 2020. Periglacial water paths within a rock glacier dominated catchment in the Stepanek area, Central Andes, Mendoza. Argentina. Permafr. Periglac. Process. 31, 311–323. https://doi.org/10.1002/ppp.2044.

Turetsky, M.R., Abbott, B.W., Jones, M.C., Walter Anthony, K., Olefeldt, D., Schuur, E.A. G., Grosse, G., Kuhry, P., Hugelius, G., Koven, C., Lawrence, D.M., Gibson, C., Sannel, A.B.K., McGuire, A.D., 2020. Carbon release through abrupt permafrost thaw. Nat. Geosci. 13, 138–143. https://doi.org/10.1038/s41561-019-0526-0.

Wang, G., Ju, Q., Guodong, C., Yuanmin, L., 2002. Soil organic carbon pool of grassland soils on the Qinghai-Tibetan Plateau and its global implication. Sci. Total Environ. 291 (1–3), 207–217.

Wayne, W.J., Corte, A.E., 1983. Multiple glaciations of the Cordon del Plata, Mendoza, Argentina. Palaeogeogr., Palaeoclim. Palaeoecol. 42 (1-2), 185–209.

Wojcik, R., Palmtag, J., Hugelius, G., Weiss, N., Kuhry, P., 2019. Land cover and landform-based upscaling of soil organic carbon stocks on the Brogger Peninsula. Svalbard. Arct. Antarct. Alp. Res 51, 40–57. https://doi.org/10.1080/15230430.2019.1570784.

Zou, D., Zhao, L., Sheng, Y., Chen, J., Hu, G., Wu, T., Wu, J., Xie, C., Wu, X., Pang, Q., Wang, W., Du, E., Li, W., Liu, G., Li, J., Qin, Y., Qiao, Y., Wang, Z., Shi, J., Cheng, G., 2017. A new map of permafrost distribution on the Tibetan Plateau. Cryosphere 11, 2527–2542. https://doi.org/10.5194/tc-11-2527-2017.